Department of Computer Science and Communications Engineering,
the Graduate School of Fundamental Science and Engineering
of Waseda University

Master's Thesis

Study on Field Experiment for Visualization of Radio Signal with UAV

January 30th, 2017

Hikari INATA

(5115F015-5)

Shimamoto Laboratory

(Professor Shigeru Shimamoto)

Abstract

In this thesis, we propose a system for visualization of radio signal using UAV in the field. We are able to measure the directivity of antennas if we use anechoic chamber. However, it is difficult to obtain the directivity of antennas in the real field. In order to get the directivity of antennas in the field, we propose the system which uses detector circuits which convert radio signals to light, received antennas, and UAV. To obtain the directivity in the field, we carry out an experiment. In this experiment, we use Yagi-antennas. The results show that precision of the system is a moderate match to the directivity obtained from the chamber. The results also confirm the proposed system is practical in the field.

Key word – UAV, Yagi-Antenna, Method of Moments, Characteristics of directivity, anechoic chamber,

Table of Contents

List of Figures

List of Tables

Chapter 1

Introduction

1.1 Background

We can illustrate the directivity of the antenna if we use the anechoic chamber. However, it is so difficult for us to illustrate the directivity of the antenna in the real fields. Knowing the directivity of the antenna becomes more important as the technology advances to 5G. As the technology enhances to 5G, along with the construction of more number of the Base Stations, optimization of the antenna becomes tedious. And it is helpful for maintenance and inspection to know the directivity of the Base Station's antenna. If the directivity of the installed antenna is known or can be forecasted, the orientation of antenna can be fixed during the implementation phase itself. This thesis proposes an experiment based visualization system in which LED lights are used to visualize and exhibit the orientation of the antenna.

Incidentally, the height of the Base Stations is high in many cases. Therefore, the maintenance of Base Station by human resources is very risky and costly. In such cases, usage of UAV makes the maintenance and construction of Base Stations less risky and efficient. In combination with the visualization system, they benefit in following ways;

- Fixing of good tilt angle of the antenna during construction becomes easier using this system.
- Regular inspection and maintenance of Base Station can be carried out using this system.

Therefore, the experiment in this thesis proves to be to be useful for future implementation in real scenarios.

1.2 Thesis Objectives

In general, we are not able to observe the directivity of antennas unless we use anechoic chamber. Most of previous studies are able to observe electric field intensity indoors or outdoors using slightly big equipment including some PCs. Due to slightly big equipment, the visualization system does not have mobility to visualize directivity of antenna which is located high altitude. Therefore, this thesis aims to be able to illustrate the directivity of antennas using small equipment and UAV having mobility. To establish the visualization system which can illustrate the directivity of antennas, I did the experiment which content is visualization of Yagi-antenna of 3 elements and of 6 elements. Furthermore, in order to confirm the success of the visualization system, I simulated the 3-dimension pattern of directivity of antennas and made a comparison between results and simulations.

1.3 UAV

Recently, it has been raised in importance about UAV which is an acronym for Unmanned Aerial Vehicle or Unmanned Automobile Vehicle. The UAV is an aircraft that flies without a human crew on board the aircraft and the UAV has so many types of small-size to large-size [1][2][3]. Principal applications of the UAV are military, conveyance, aerial photography, disaster investigation [4][5], and etc. And in the United States, the UAV are used by military in most other cases. For instance, the UAV has been used as a reconnaissance plane which name is Global Hawk in United States of America and Figure 1.1 shows the Global Hawk.

Figure 1.1 Global Hawk (From a homepage of Northrop Grumman Company) [6]

And recently, we often watch an aerial photography or moving image on television due to the progress of the UAV. The UAV can be roughly classified into type of fixed wing and type of rotary wing. The previously described Global Hawk is type of fixed wing, and UAV which is used by aerial photography and moving image is often type of rotary wing. The PHANTOM2 and INSPIRE from DJI Co., Ltd are famous as the UAV which type is rotary wing. The PHANTOM2 is shown Figure 1.2 and INSPIRE is shown Figure 1.3.

Figure 1.2 PHANTOM2

Figure 1.3 INSPIRE

Major characteristics of type of rotary wing is that UAV can hover. Hovering means that UAV can remain at a particular position (height or state) for a long period of time. Therefore, type of rotary wing is better than type of fixed wing for measurement of propagation characteristics of electromagnetic wave or bit error rate. In this thesis, I used the UAV which type is rotary wing for experiment.

1.4 Utilization condition of UAV

In 2011, the Fukushima No.1 nuclear power plant stopped. We could not investigate by human due to radioactive contamination. The Global Hawk which has United States was used to investigate the disaster damage condition and the nuclear reactor condition. The Global Hawk is the UAV which can be staying in high altitude. The Global Hawk was developed by Northrop Grumman Company in the United States for gathering information and reconnaissance. The Global Hawk has some radars and cameras for data collection or investigation. In the United States, the UAV are used by military in most other cases. The Global Hawk does not have offensive capability, but There are UAVs which have missiles for military defense. In addition, the UAVs are used for transport and communication when disasters occur in the United States.

In Japan, UAVs were used to distribute agrochemical efficiently over a paddy field. However, in recent years, the UAVs are used for not only agricultural sector but also observation of volcanic activities in Mt. Usu, Miyake island, etc. And the UAVs are also used to investigate condition of bridges. In Japan where is likely to experience many disasters including the Great East Japan Earthquake, the usage of UAV for investigation of the environment which people hardly to go is increasing. Not only in Japan but overseas, recently, we often watch the moving image from the sky on TV or movie. The UAV is also used in media sector.

And Shimamoto Laboratory has not only UAV of type of rotary wing but also UAV of type of fixed wing. This type of UAV is used for study on Unmanned Aerial Vehicle based missing detection system employing phased array antenna. And this UAV is shown as Figure 1.4.

Figure 1.4 Shimamoto Lab's UAV which type is fixed

1.5 Thesis Organization

The organization of the chapter is as follows:

- ✓ Chapter 1 (Introduction) gives the background and motivation of this thesis.
- ✓ Chapter 2 (Overview of System Architecture) introduces the details of our system architecture.
- ✓ Chapter 3 (Experiment Set Up) introduces the details of our system architecture.
- ✓ Chapter 4 (Simulation) shows our simulation scenario and results.
- ✓ Chapter 5 (Conclusion and Future Works) summarizes our research. Moreover, rooms for improvement and future directions are discussed.

Chapter 2

Overview of System Architecture

In order to visualize the directivity of antennas, we proposed the system which is contained detector circuits, received antennas, and UAV. In this chapter, we introduce system configurations which is using in this experiment in detail.

2.1 Detector Circuit

In order to construct the visualization system, we installed the detector circuit. The detector circuit detects the radio waves. Specifically, the type of detector circuits is half-wave double-voltage rectifier circuit which diagram is shown as Figure 2.1. The half-wave double-voltage rectifier circuit consists of two circuits: a clamper circuits which is shown as Figure 2.2 and peak detector (half-wave rectifier) which is shown as Figure 2.3. Now I would like to explain mechanism of the half-wave double-voltage rectifier circuit. On the negative half cycle of AC input, C1 charges. During the positive half cycle, the half-wave rectifier comes into play. Diode D1 is out of the circuit because it is reverse biased. Now C1 is in series with the voltage source. Note the polarities of the generator and C1, series aiding. Thus, DC mater displays double-voltage [7]. For instance, when input voltage is 5V, DC mater indicates about 10V. In this system, we use the detector

circuits applying the half-wave double-voltage rectifier circuit. This detector circuit diagram is illustrated as Figure 2.4. This circuit is composed of half-wave double-voltage rectifier circuit, resisters, and LED light. The circuit catches the radio wave from the connected antenna, and the current flows in the LED right. If the radio wave strength which is received by this circuit is low, LED light shines weakly and vice versa [8].

We assembled the visualization circuits is shown as Figure 2.5, and Figure 2.6 shows the changes of light intensity which accompany distance from received antenna to transmitted antenna.

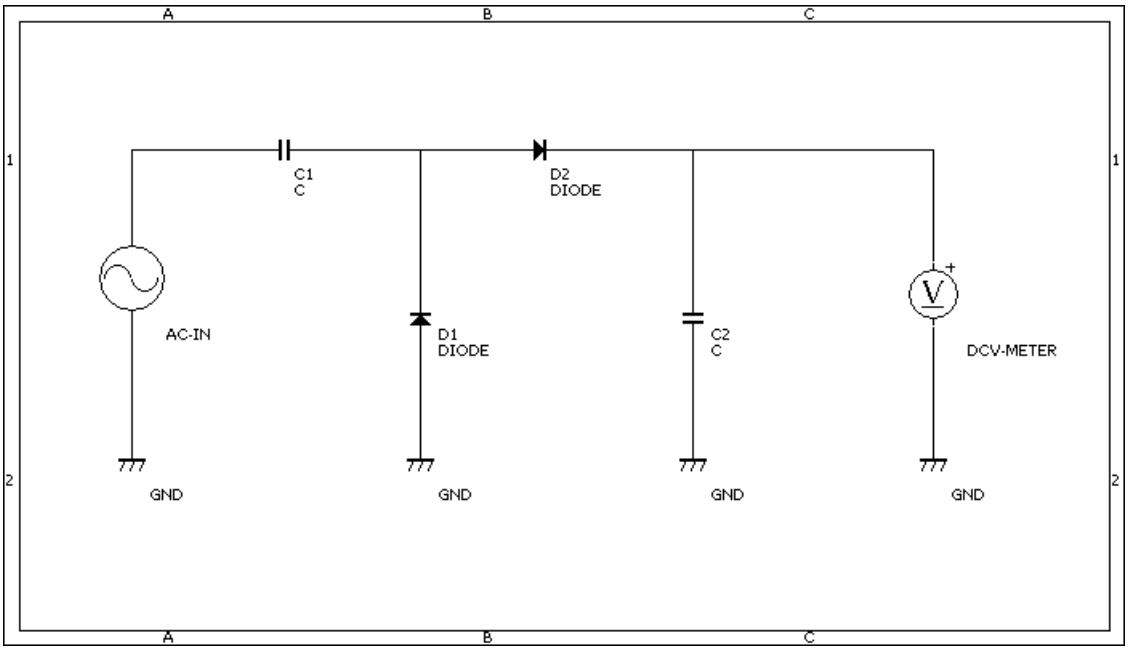

Figure 2.1 half-wave double-voltage rectifier circuit

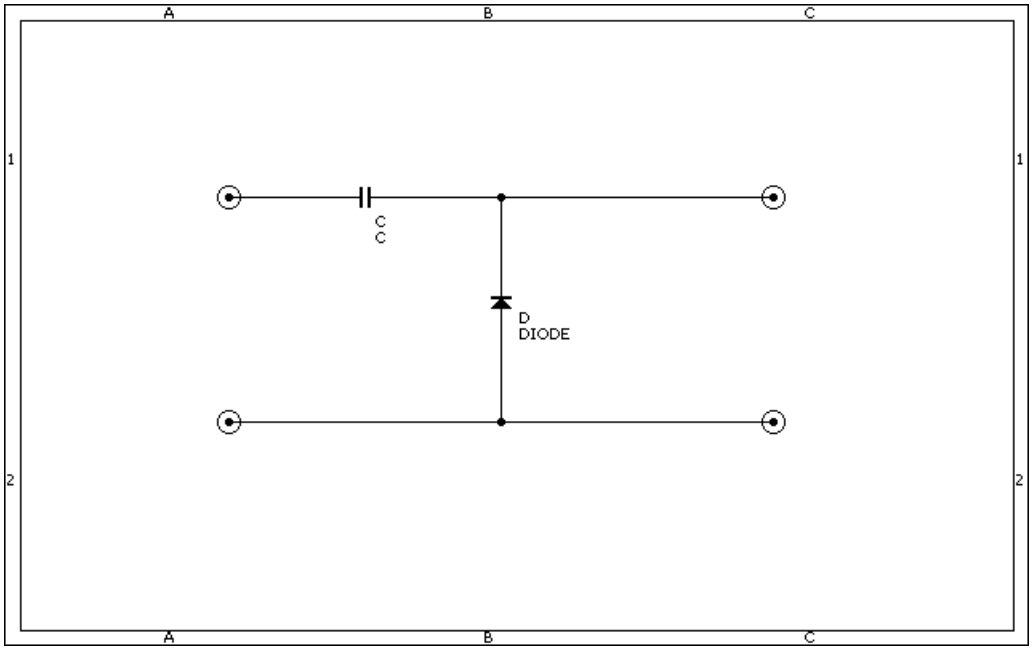

Figure 2.2 clamper circuit

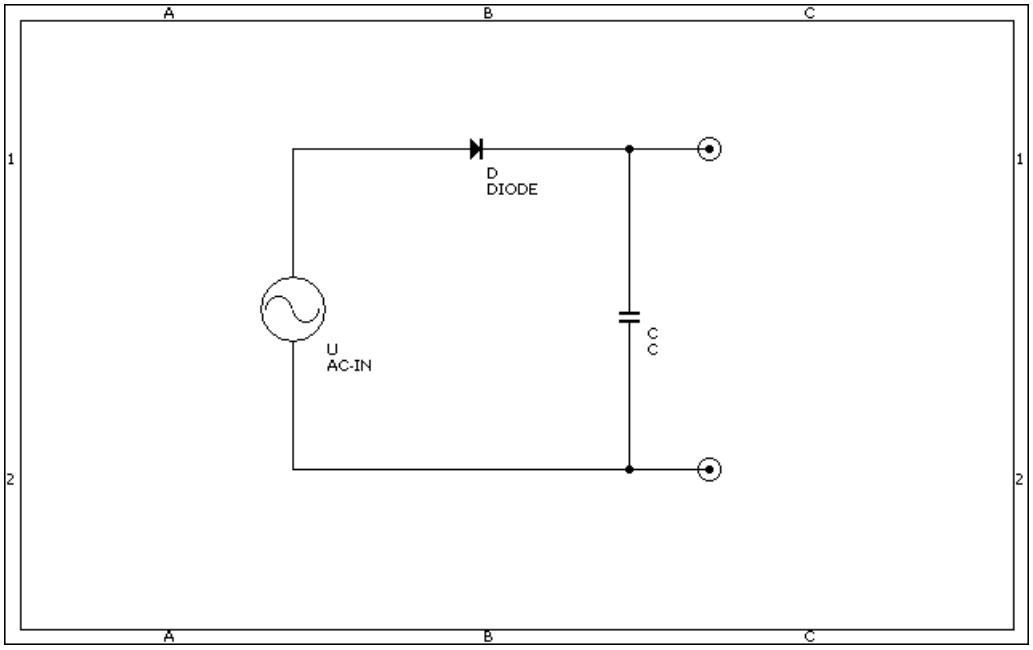

Figure 2.3 half-wave rectifier circuit

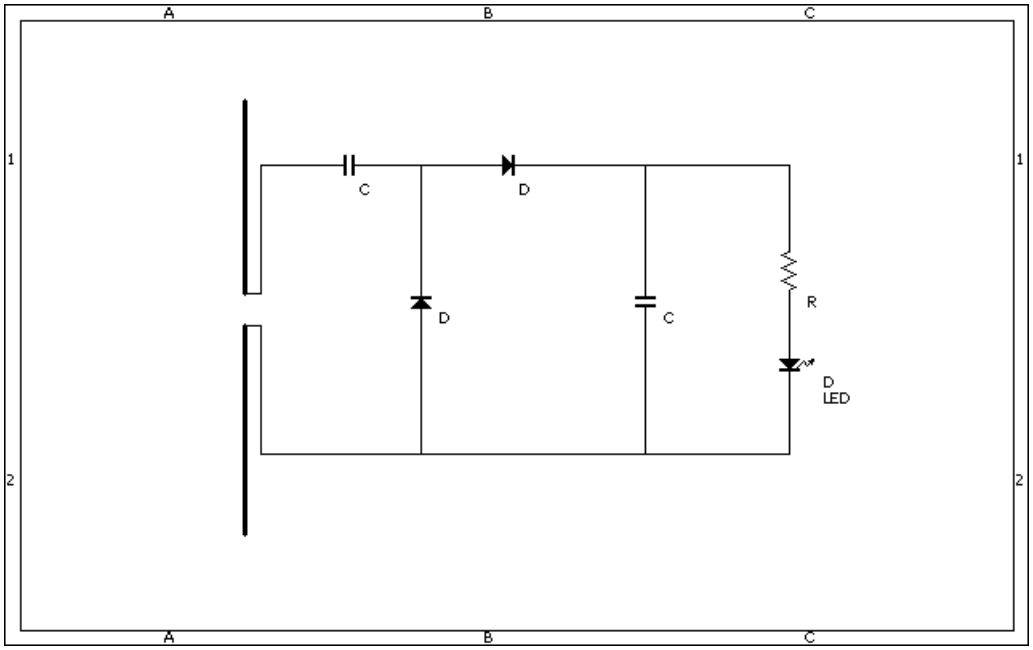

Figure 2.4 visualization circuit

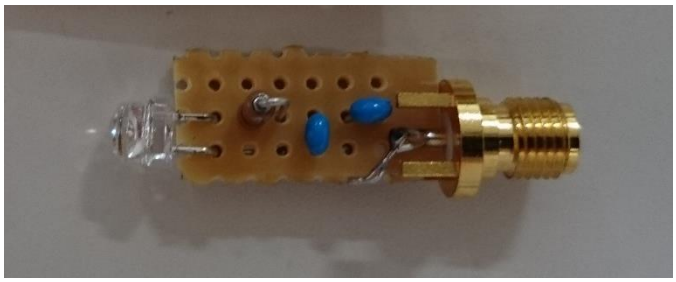

Figure 2.5 the assembled visualization circuit

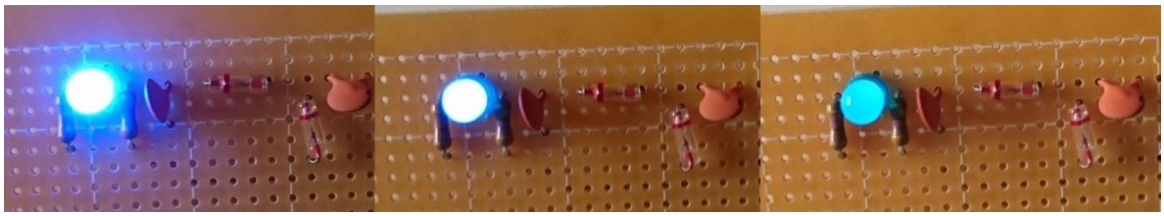

Figure 2.6 changes of light intensity which accompany distance

2.2 Dipole Antenna

In order to construct the visualization system, we have to use and make the received antennas. We use the antennas which type is center-fed half-wave dipole which is shown as Figure 2.7 in the system. The half-wave dipole has been the most popular antenna used by amateurs worldwide, largely because it is very simple to construct and because it is an effective performer [9][10]. It is also a basic building block for many other antenna systems, including beam antennas, such as Yagi antennas[11][12].

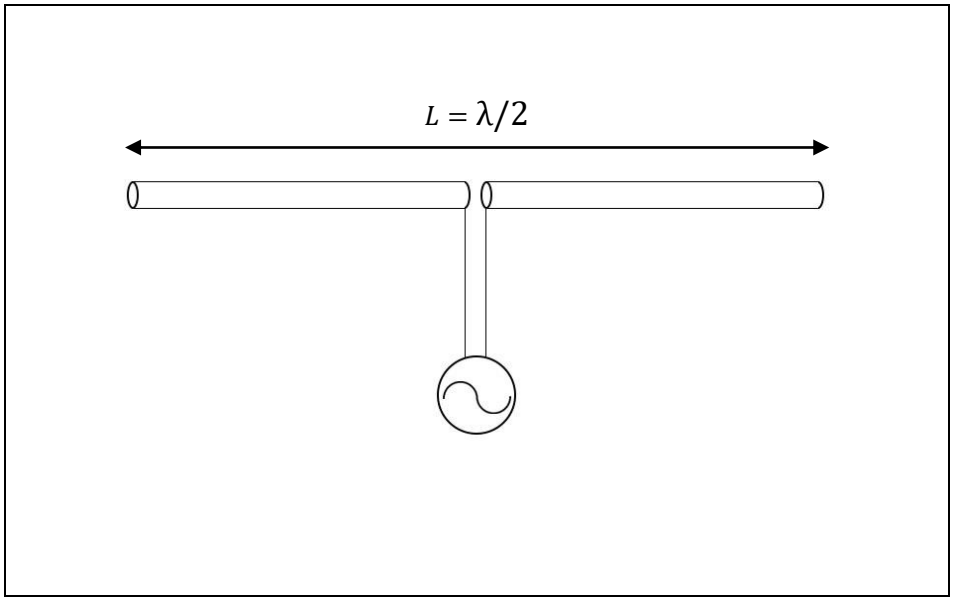

Figure 2.7 center-fed half-wave dipole

A center-fed half-wave dipole antenna consists of two elements, and

fed. The length of element is one-half wavelength long as defined in the following formula 2.1.

$$\lambda = \frac{c}{f} \tag{2.1}$$

Where λ is wavelength, c is speed of light, and f is frequency. In free space, the theoretical impedance of a physically half-wave long antenna made of an infinitely thin conductor is $73 + j42.5\ \Omega$. This means this antenna exhibits resistance and reactance.

In this system, we use the center-fed half-wave dipole antennas as a received antenna. The material of two elements is aluminum. We cut aluminum poles into required length which can be obtained by formula 2.1. For instance, when the frequency is 435[MHz], and speed of light is about $3.0 \times 10^8 [m/s]$, the one wavelength are obtained by formula 2.1. The one wavelength λ is ;

$$\begin{aligned} \lambda &= \frac{3.0 \times 10^8}{4.35 \times 10^8} [m] \\ &\approx 0.69 \qquad [m] \end{aligned}$$

From this one wavelength, we can obtain the length of elements by dividing λ with 4. Then, we are able to obtain the length of elements which is about 17.25[cm].

Next, I explain about how to join two elements with a coaxial cable.

One element needs to connect a center core of a coaxial cable, and the other needs to connect a shield of a coaxial cable. A structure of coaxial cable is illustrated as Figure 2.8. To connect two elements with a coaxial cable, a center core and a shield have to separate. After separation of a center core and a shield, the crimp terminals are mounted on the center core wire and a shield wire end part, and is shown as Figure 2.9. Moreover, it is necessary for elements to make a hole using a drill to turn a screw. Finally, we connect elements with the center core wire and the shield wire which are added crimp terminals by using a screw.

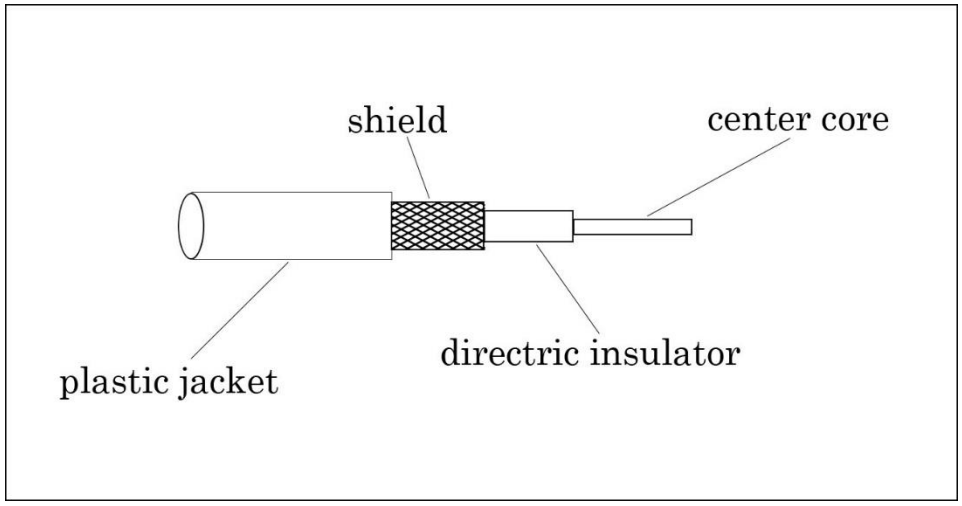

Figure 2.8 structure of coaxial cable

Figure 2.9 connection of crimp terminals with center core and shield

2.3 UAV

To assemble the visualization system, we installed the UAV which type is rotary wing. We choose the UAV which type is rotary because this type is able to do hovering. Type of fixed wing is able to put on more speed than type of rotary wing, but it is difficult for fixed one to keep same position. However rotary wing can be hovering, so we chose the rotary wing for the visualization system to obtain data.

In order to implement the visualization system, we have to know payload of the UAV. Payload means the total weight of equipment carried by an aircraft. I would like to show the specific of UAV which name is INSPIRE 1 and is used in the system in table 2.1.

TABLE 2.1 Specification of UAV which is used in the system [13]

Weight	3060g(including propellers, battery and gimbal)
Maximum Ascent Speed	5m/s
Maximum Descent Speed	4m/s
Maximum Speed	79km/h(no wind)
Maximum Wind Speed Resistance	10m/s
Maximum Flight Time	18min
Maximum Takeoff Weight	3500g
Operating Temperature	-10 – 40 Celsius Degree

According to the specification of INSPIRE 1 in table 2.1, the payload of INSPIRE 1 is 440g when UAV loads the battery and gimbal. So we have to make the system weighting less than 3500g and weight of parts of detectors and received antennas is less than 440g. We assembled the visualization system within the permissible range and this system using UAV which name is INSPIRE 1 is shown as Figure 2.10.

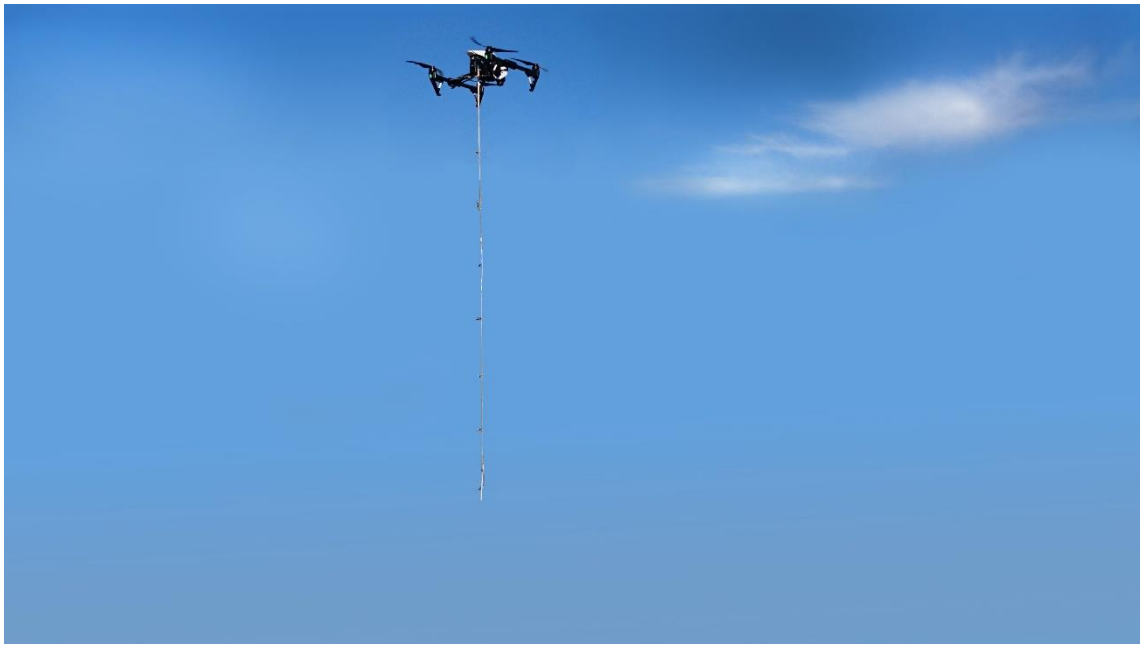

Figure 2.10 visualization system using INSPIRE 1

Chapter 3

Contents of Experiment

To visualize the radio signal from antennas, we have to implement the visualization system. In order to implement this and visualize the directivity, we carried out some experiment. In this chapter, we introduce the contents of experiment.

3.1 Measurement of Antennas

We used some antennas which name are dipole antenna and Yagi antenna. Dipole antennas were used in the visualization system, and Yagi antennas which have 3 elements and 6 elements were used as antennas under test. For implementation of the system, it is so important for characteristics of those antennas. Thus, we need to know whether the characteristics of those antennas are within the permissible range. So we measured the characteristics of dipole antennas and Yagi antennas. The measurement characteristics are VSWR and directivity. VSWR is acronym for Voltage Standing Wave Ratio, and VSWR is also referred to as Standing Wave Ratio (SWR). The VSWR is the ratio of the maximum voltage (resulting from the interaction of incident and reflected voltages along the line) to the minimum voltage. This is a function of the reflection coefficient, which describes the power reflected from the antenna [14]. If the voltage of

progressive wave is given as V_f, and the voltage of reflected wave is given as V_r, then the VSWR is defined by the following formula 3.1 and 3.2:

$$VSWR = \frac{|V_f| + |V_r|}{|V_f| - |V_r|} \tag{3.1}$$

$$= \frac{1 + \left|\frac{V_r}{V_f}\right|}{1 - \left|\frac{V_r}{V_f}\right|}$$

$$VSWR = \frac{1 + |\Gamma|}{1 - |\Gamma|} \tag{3.2}$$

Where Γ is V_r/V_f, and Γ means the reflection coefficient. The reflection coefficient is also known as S11 (S-parameter) or related to return loss. S11 represents how much power is reflected from the antenna. And the return loss is the loss of power in the signal reflected by a discontinuity in a transmission cable. The return loss is usually expressed as a ratio in decibels. If incident power is given as P_f, reflected power is given as P_r, then the return loss is defined by the following formula 3.3;

$$Return\ \ Loss\ \ [dB] = 10 \log_{10} \frac{P_r}{P_f} \tag{3.3}$$

Method of measurement for directivity is using the anechoic chamber and calculation soft wear which name is TOYO 2100AM. So we

measured the directivity of antennas using these. And, method of measurement for S11 (VSWR) is using antenna analyzer which name is AA-1400 which is shown as Figure 3.1. This antenna analyzer is able to measure the SWR, return loss, and smith chart. So in this experiment, we measured the VSWR using this antenna analyzer.

Figure 3.1 antenna analyzer (AA-1400)

3.2 Experiment about Visualization of Directivity

We carried out the experiment to visualize the directivity of antennas which is Yagi antenna using UAV in the real field. And Figure 3.2 shows the image of experiment. At first, measured 3 elements Yagi antenna is located at 2 m. And we connect the measured antenna with transmitter which name. After this, we turn on power to the UAV of the system and move the UAV of the system linearly from 0m to 7m. Then we take a photography about this in a consecutive shot mode. We obtain the data 5 dimension in this way. Figure 3.3 shows the diagram of how to get the data in this experiment. Number 1 to 5 in Figure 3.3 means measurement dimension. If we finish to obtain the data about 3 elements Yagi antenna, next we move on to measure 6 elements Yagi antenna in this way.

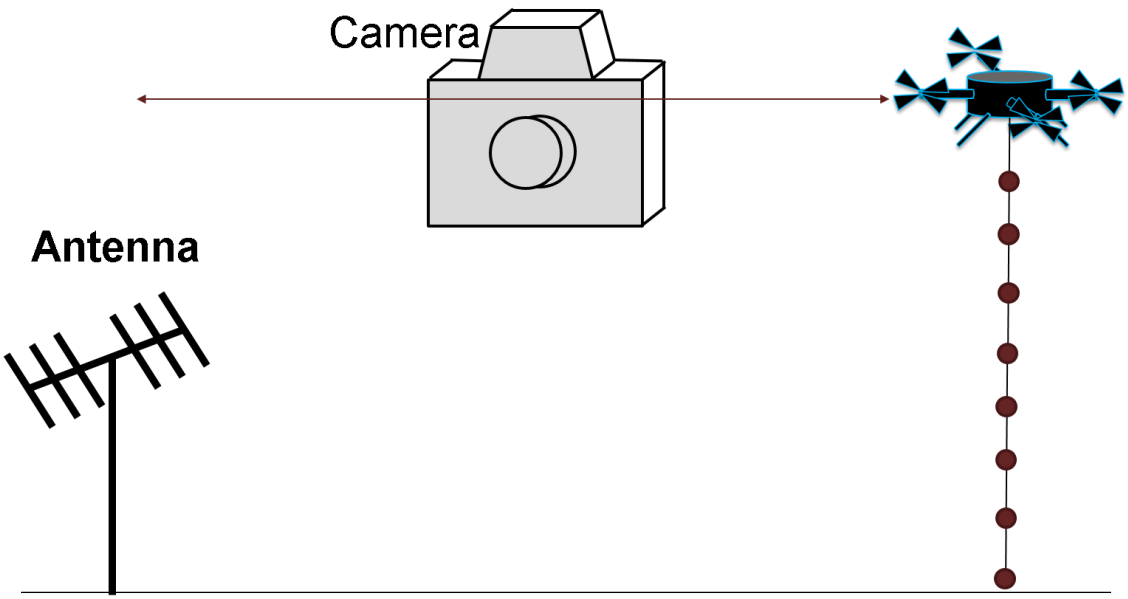

Figure 3.2 image of experiment

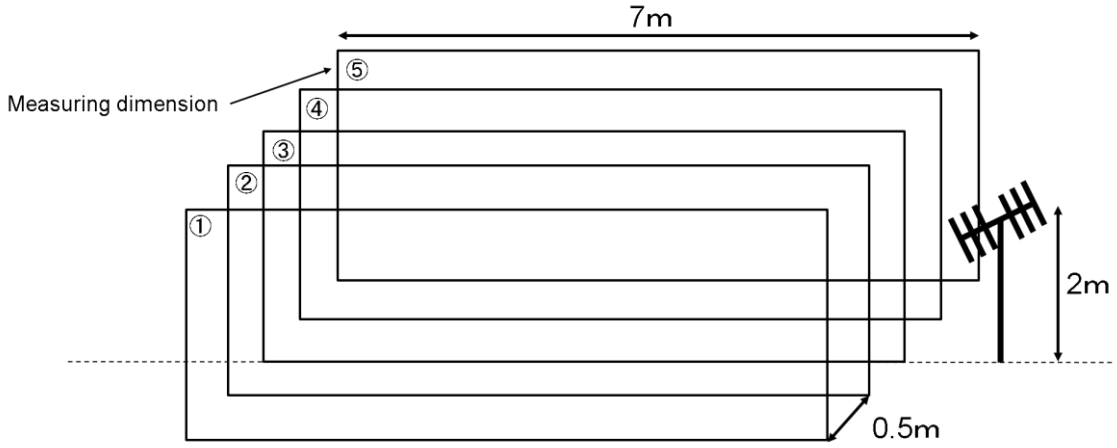

Figure 3.3 diagram of how to get the data

And table 3.1 means the parameters of experiment. Weather is sunny and wind speed is 4.0 m per second.

TABLE 3.1 parameters of experiment

Transmitted Power	20 [W]
Frequency	435.81 [MHz]
Height of Antenna	2.0 [m]
Number of elements (Yagi ant.)	3
	6
Measured Distance	7.0 [m]
Measuring dimension interval	0.5 [m]

Chapter 4

Results

4.1 Dipole Antenna

We measured the characteristics of VSWR, Return Loss, and directivity of making dipole antennas using antenna analyzer AA-1400 is shown as Figure 3.1. At first, we show the characteristics of SWR and Return Loss of 8 dipole antennas which is used in the visualization system. Figure 4.1 is shown as SWR and Return Loss of dipole antenna 1. Figure 4.2 is shown as SWR and Return Loss of dipole antenna 2. Figure 4.3 is shown as SWR and Return Loss of dipole antenna 3. Figure 4.4 is shown as SWR and Return Loss of dipole antenna 4. Figure 4.5 is shown as SWR and Return Loss of dipole antenna 5. Figure 4.6 is shown as SWR and Return Loss of dipole antenna 6. Figure 4.7 is shown as SWR and Return Loss of dipole antenna 7. Figure 4.8 is shown as SWR and Return Loss of dipole antenna 8.

As we mention before section, VSWR is related to Return Loss. Then, using relationship voltages, Currency, Resister, and Power:

$$P = IV = \frac{V^2}{R}$$

Then, progressive power is given P_f, reflected power is given P_r, the ratio of P_r to P_f is expressed as:

$$\frac{P_r}{P_f} = \frac{\frac{{V_r}^2}{R}}{\frac{{V_f}^2}{R}} = \frac{{V_r}^2}{{V_f}^2} = \left(\frac{V_r}{V_f}\right)^2$$

$$\frac{P_r}{P_f} = \Gamma^2 \tag{4.1}$$

And then, using formula 3.1 and 3.3 and 4.1, Return Loss expressed as follow formula:

$$Return\ \ Loss\ \ [dB] = 10\log_{10}\Gamma^2$$

$$Return\ \ Loss\ \ [dB] = 10\log_{10}\left(\frac{VSWR-1}{VSWR+1}\right)^2 \tag{4.2}$$

We are able to express Return Loss to VSWR is shown as formula 4.2. That is why, VSWR is related to Return Loss, and reflection coefficient. Moreover, we are able to express power efficiency (T [%]) using above formulas.

$$T[\%] = (1-\Gamma^2) * 100 \tag{4.3}$$

We calculated the power efficiency of those antennas using formula 4.3. And this result is shown as table 4.1.

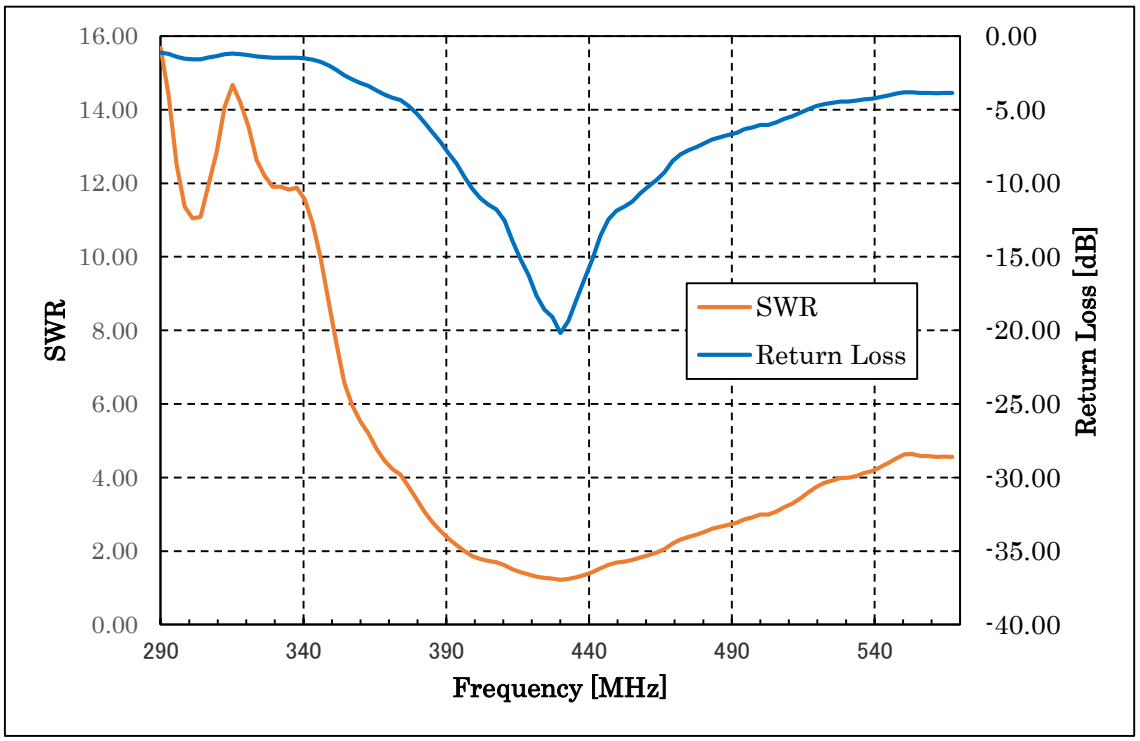

Figure 4.1 SWR and Return Loss of dipole antenna 1

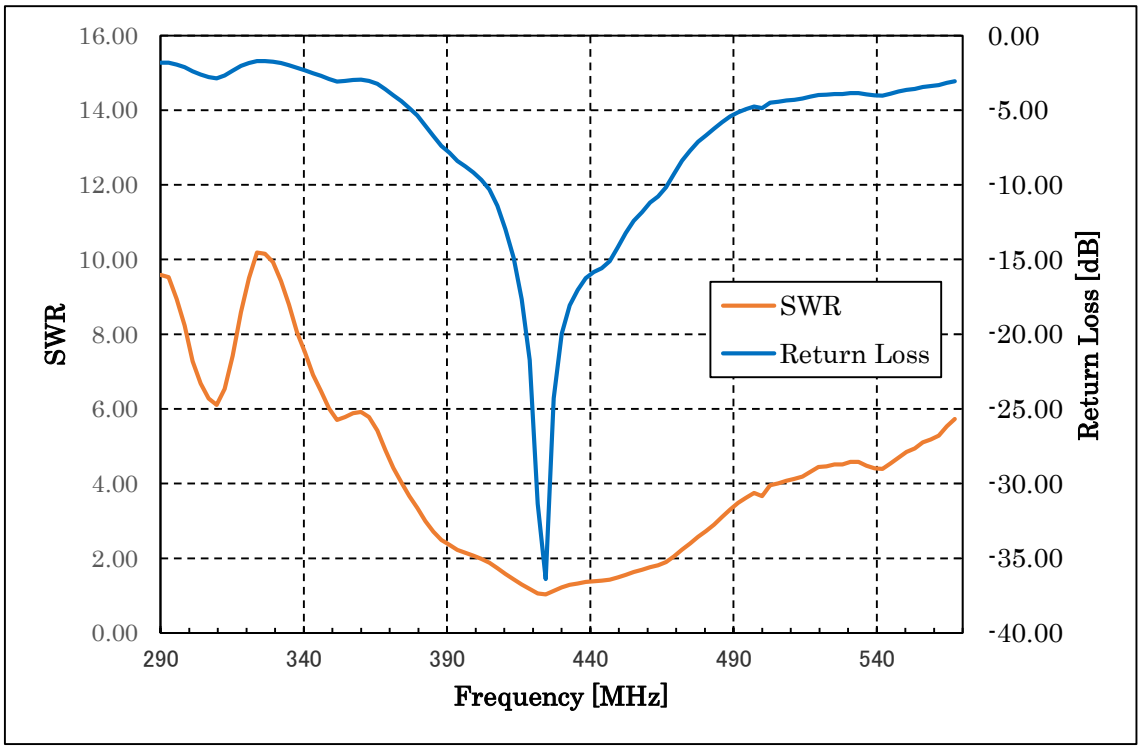

Figure 4.2 SWR and Return Loss of dipole antenna 2

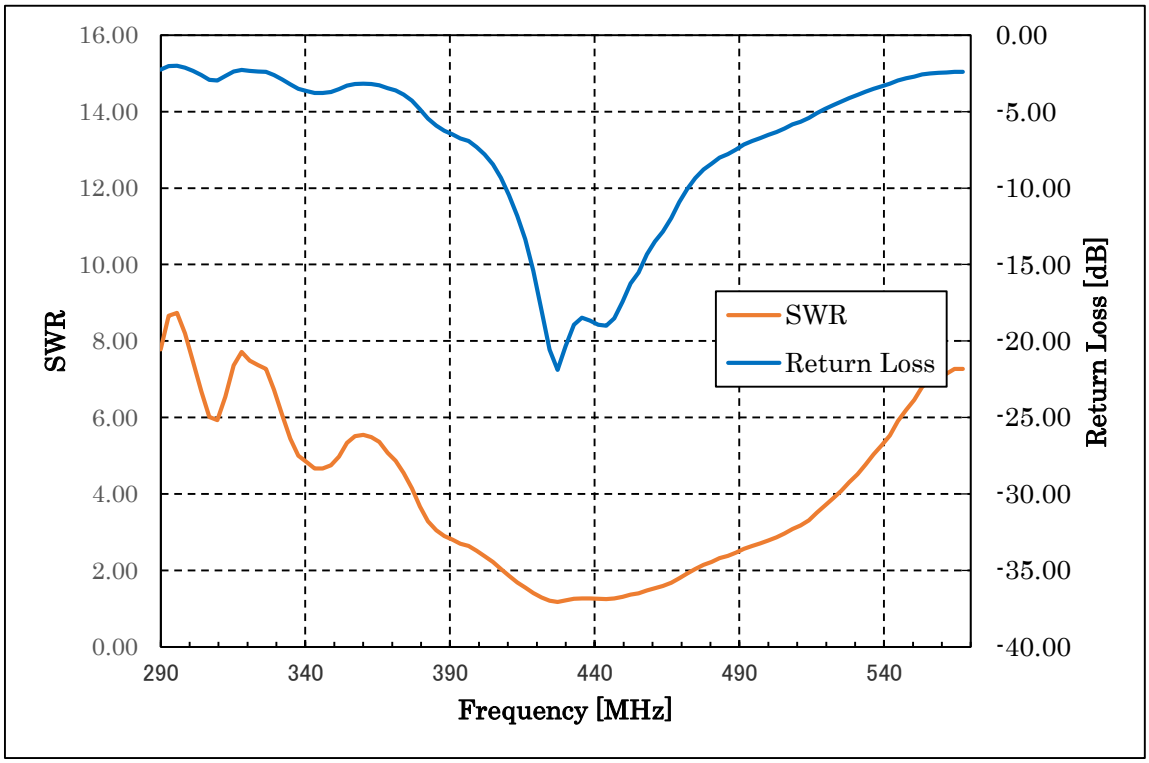

Figure 4.3 SWR and Return Loss of dipole antenna 3

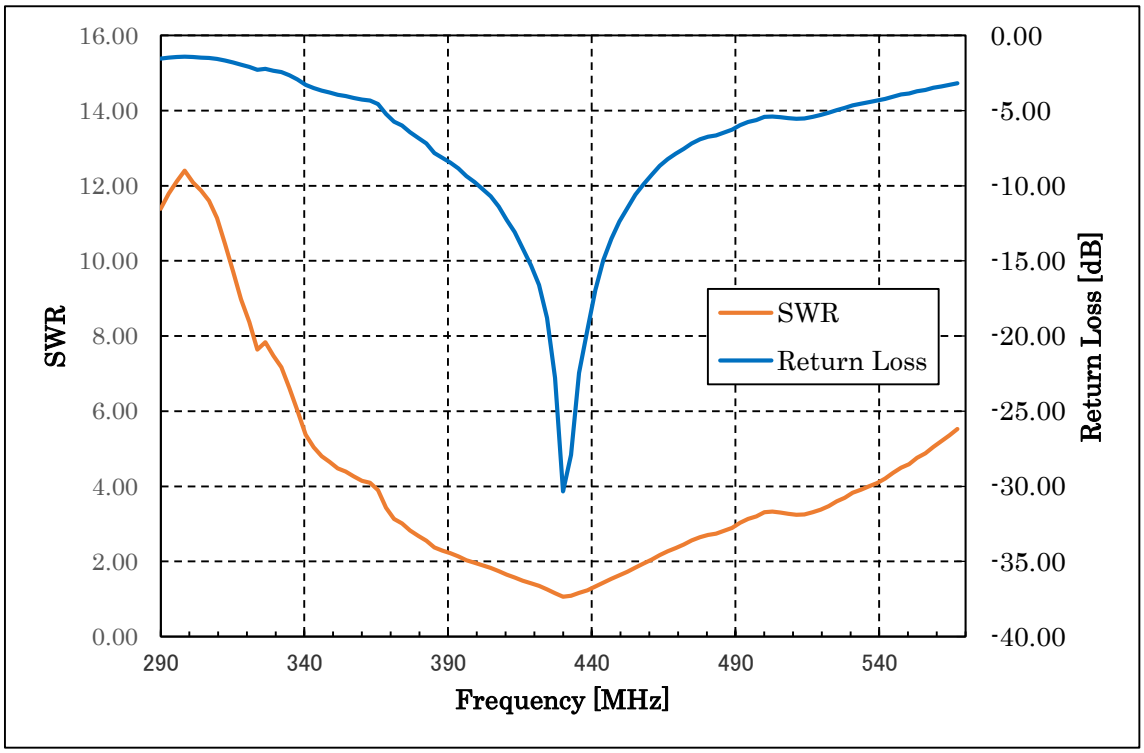

Figure 4.4 SWR and Return Loss of dipole antenna 4

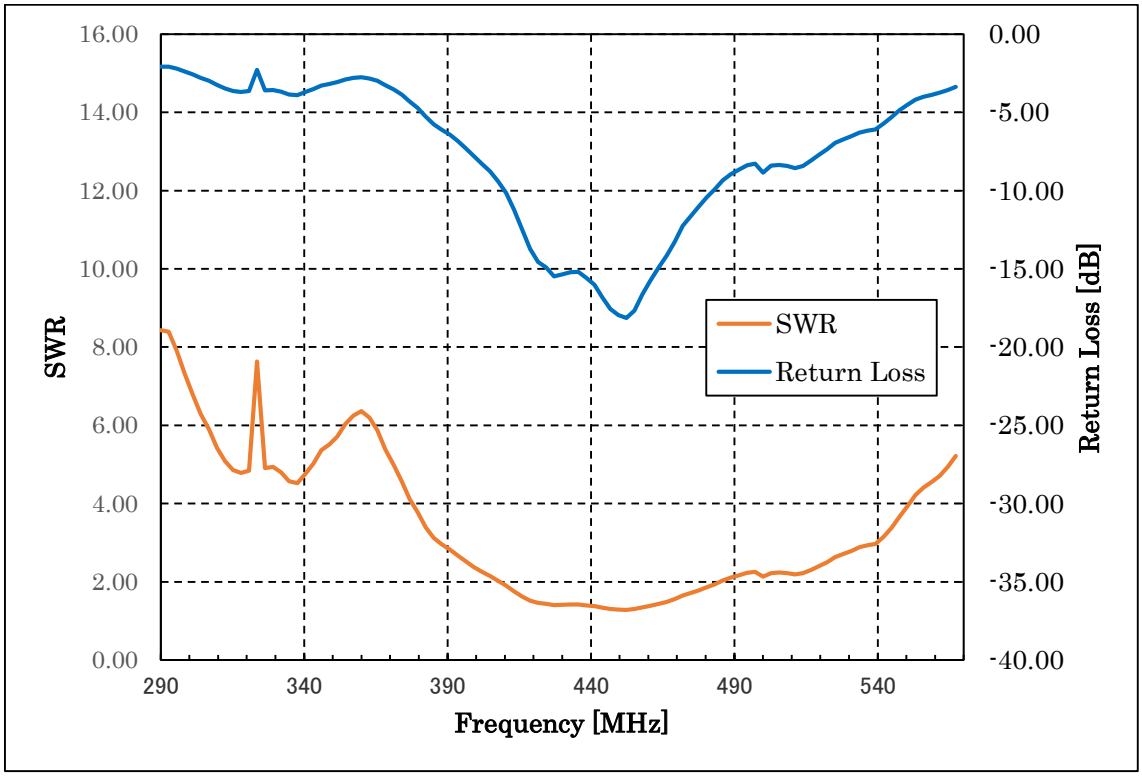

Figure 4.5 SWR and Return Loss of dipole antenna 5

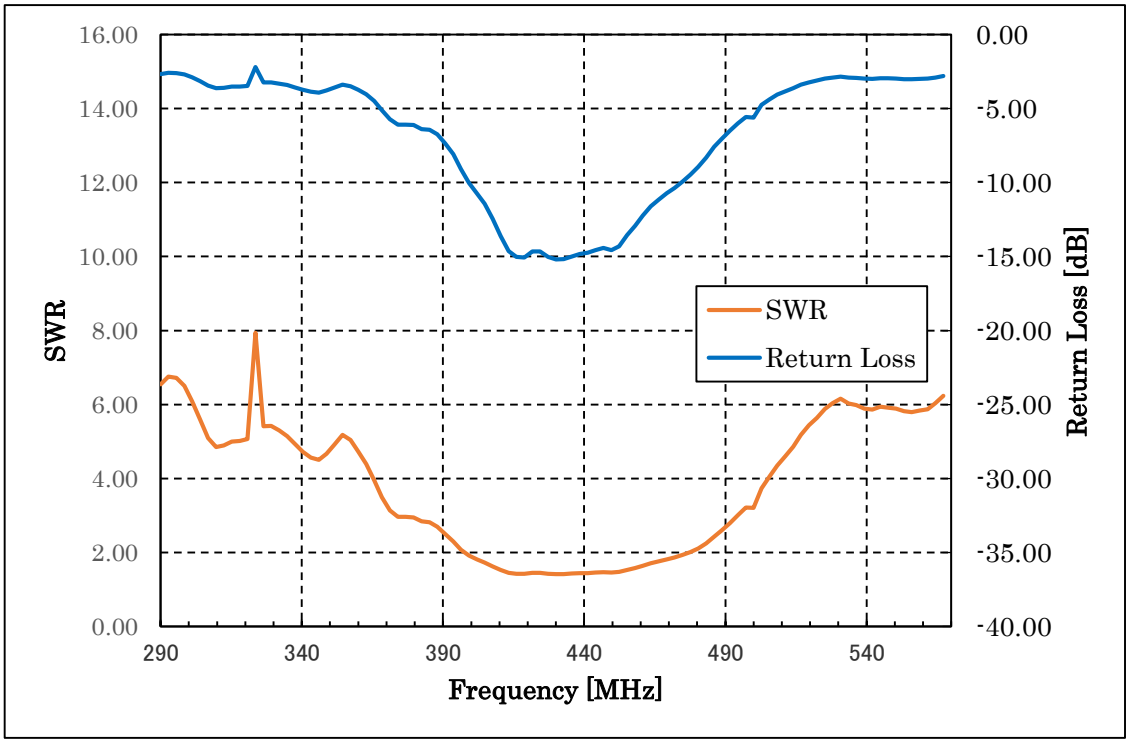

Figure 4.6 SWR and Return Loss of dipole antenna 6

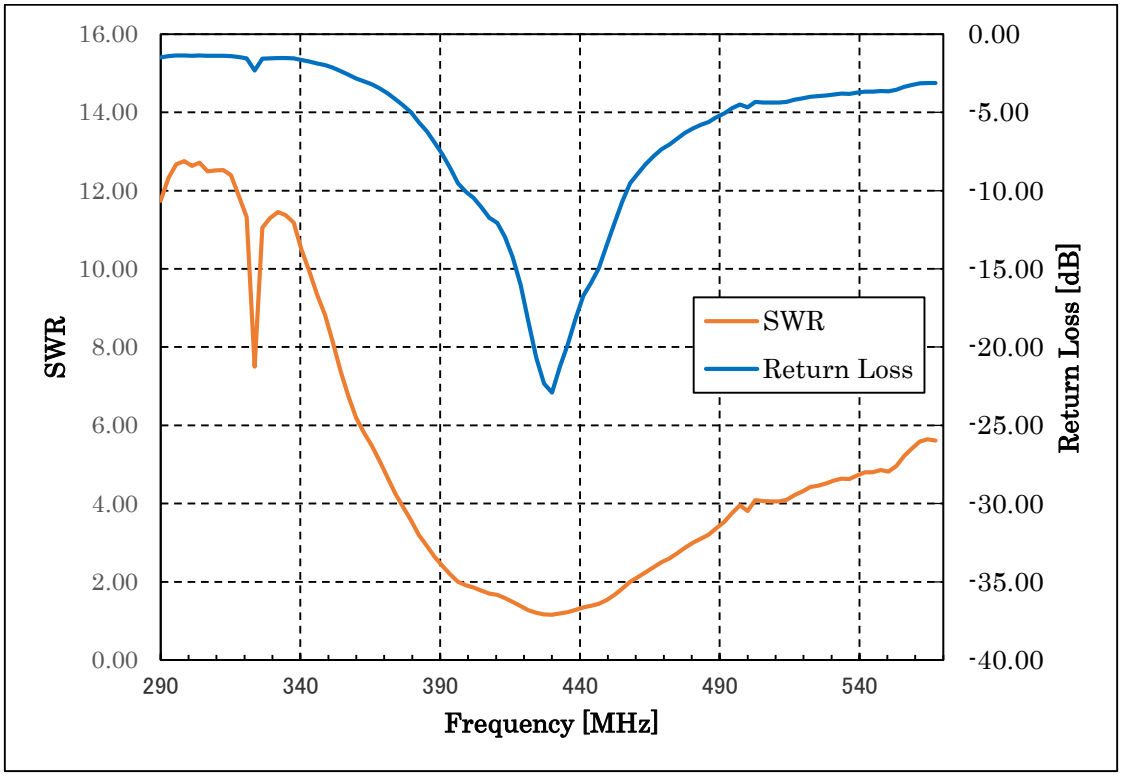

Figure 4.7 SWR and Return Loss of dipole antenna 7

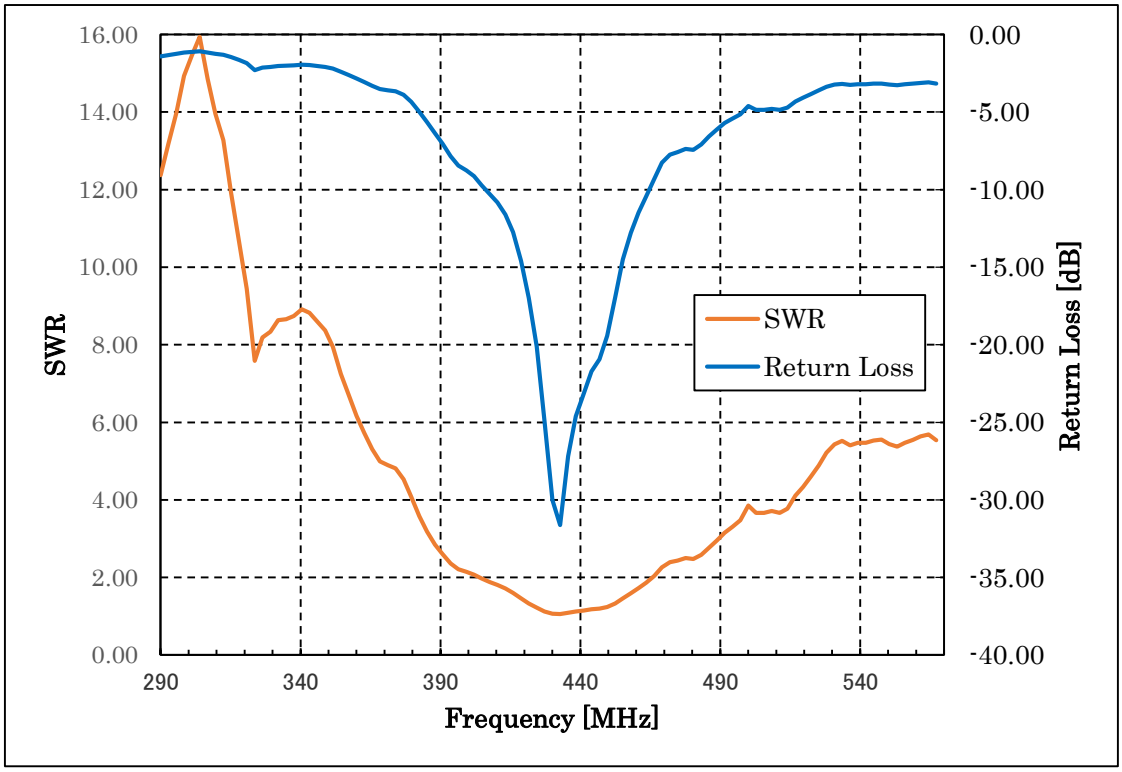

Figure 4.8 SWR and Return Loss of dipole antenna 8

TABLE 4.1 power efficiency of making dipole antennas

Number of antenna	Power Efficiency [%]
1	98.40
2	97.99
3	98.59
4	99.45
5	96.99
6	97.11
7	98.94
8	99.81

As we can see this table 4.1, we are able to confirm that the power efficiencies of those antenna are more than 96.9 percent. So, those antennas which were made by us are confirmed that those operate efficiently.

We would like to introduce the results of directivity. At first, we show the directivity of dipole antenna. Figure 4.9 shows the directivity of dipole antenna.

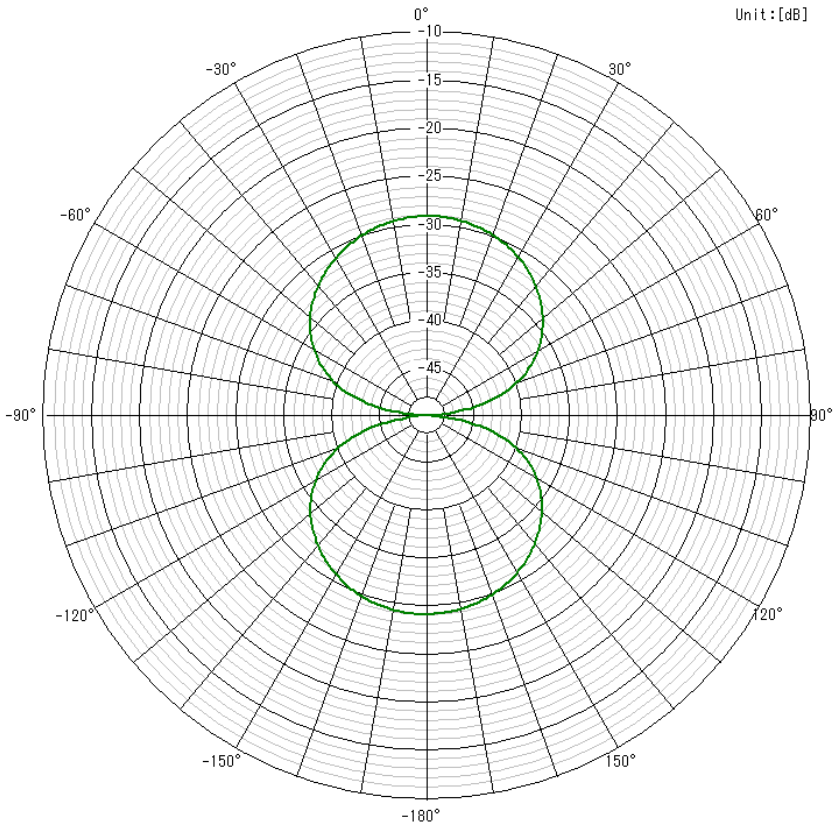

Figure 4.9 directivity of dipole antenna

4.2 Yagi Antenna

Next, we show the SWR and Return Loss of Yagi antennas. Figure 4.10 mentions SWR and Return Loss of 3 elements Yagi antenna, and Figure 4.11 is SWR and Return Loss of 6 elements Yagi antenna.

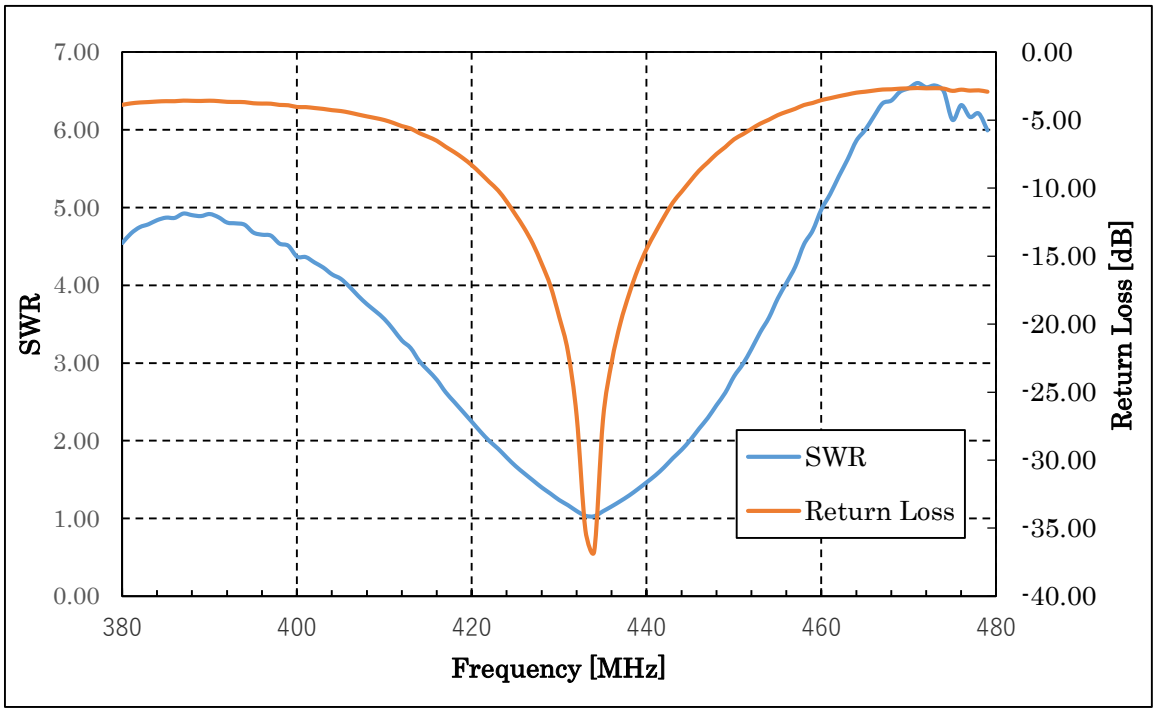

Figure 4.10 SWR and Return Loss of 3 elements Yagi antenna

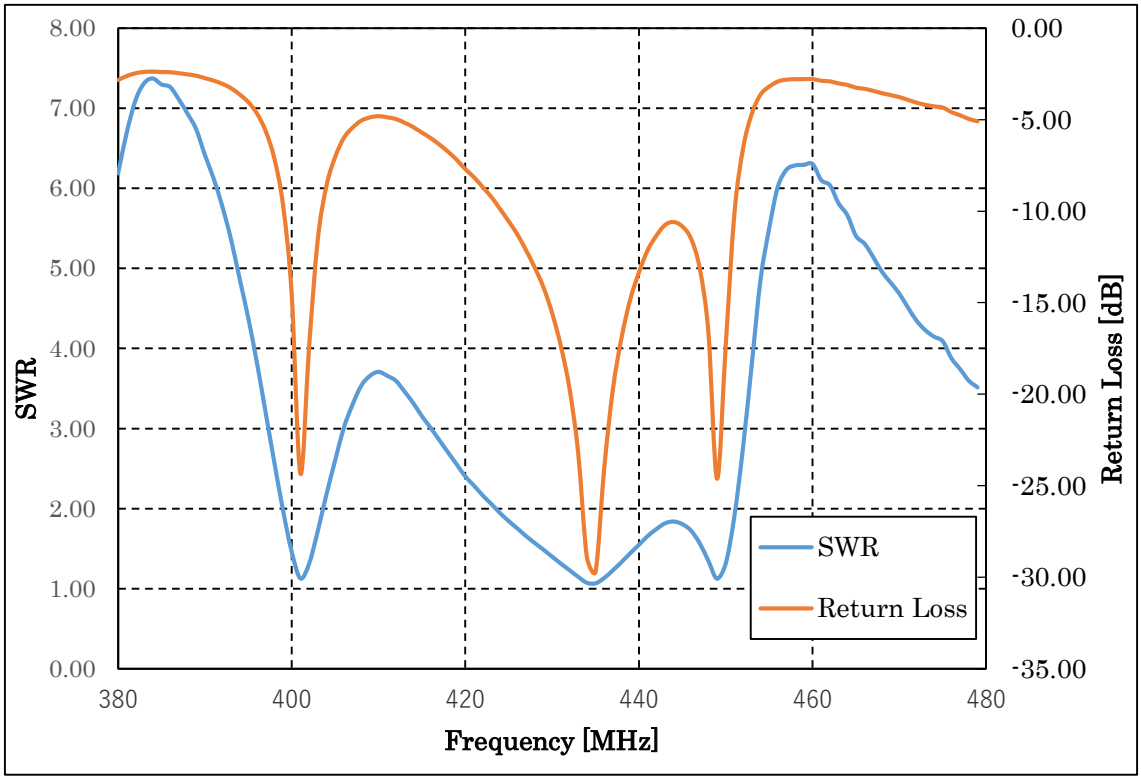

Figure 4.11 SWR and Return Loss of 6 elements Yagi antenna

Figure 4.12 shows the directivity of 3 elements Yagi antenna, and Figure 4.13 shows the directivity of 6 elements Yagi antenna.

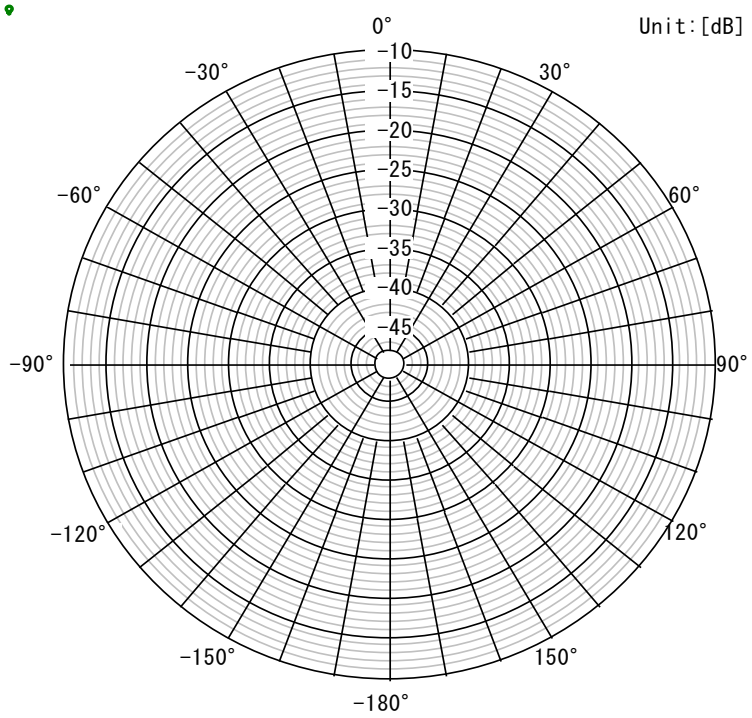

Figure 4.12 directivity of 3 elements Yagi antenna

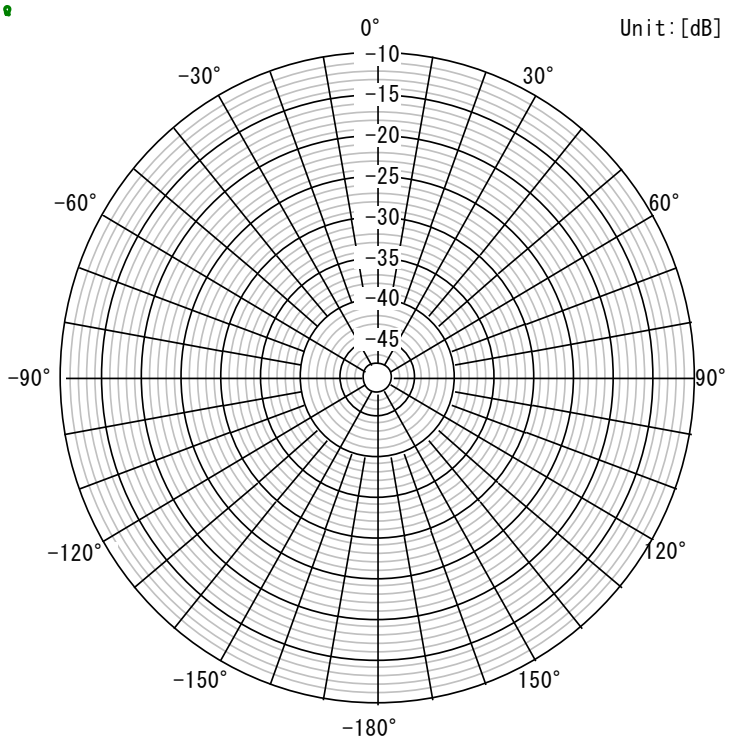

Figure 4.13 directivity of 6 elements Yagi antenna

And this results of directivity are illustrated as logarithmic scale (decibel [dB]). However, results of visualization experiment are expressed as linear scale. Due to this, we are not able to compare the data which is obtained in anechoic chamber with the data which is obtained in the visualization experiment. That is why, we should change the directivity which unit is decibel into linear. Then the unit of received power is usually in decibel-watt or decibel-milliwatt. The power in decibel-milliwatts (P_{dbm}) is equal to 10 times base 10 logarithm of the power in milliwatts (P_{mW}):

$$P_{dbm} = 10 \log_{10} \frac{P_{mW}}{1[mW]}$$

The power in milliwatts (P_{mW}) is equal to 1 [mW] times 10 raised by the power in decibel-milliwatts (P_{dBm}) divided by 10:

$$P_{mW} = 10^{\frac{P_{dBm}}{10}} \tag{4.4}$$

Using this forumula 4.4 enable to change power in decibel to in linear. And we obtained the directivity which unit is milliwatts using this formula. Figure 4.14 shows the directivity of 3 elements Yagi antenna in linear scale, and figure 4.15 shows the directivity of 6 elements Yagi antenna in linear scale.

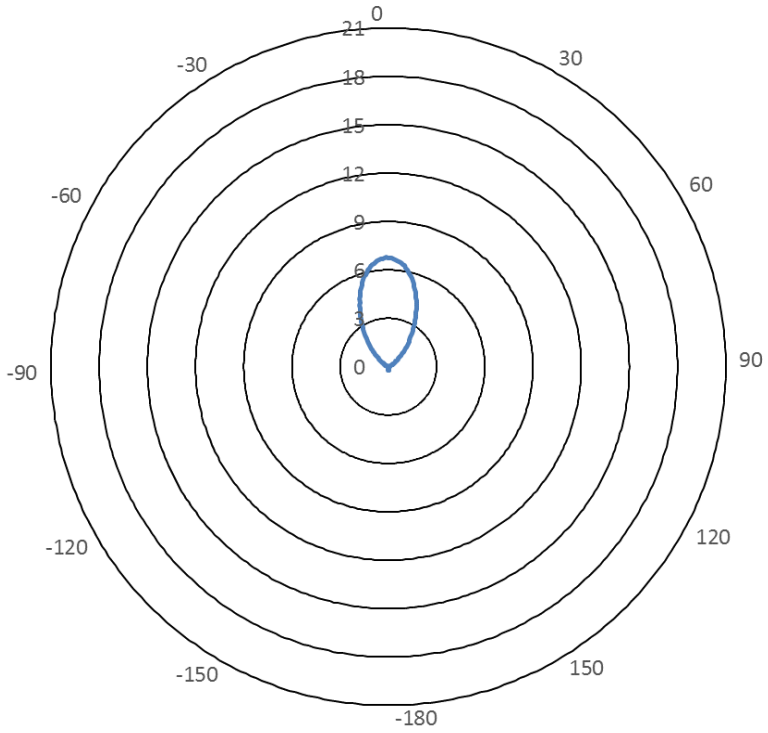

Figure 4.14 directivity of 3 elements Yagi antenna in linear scale

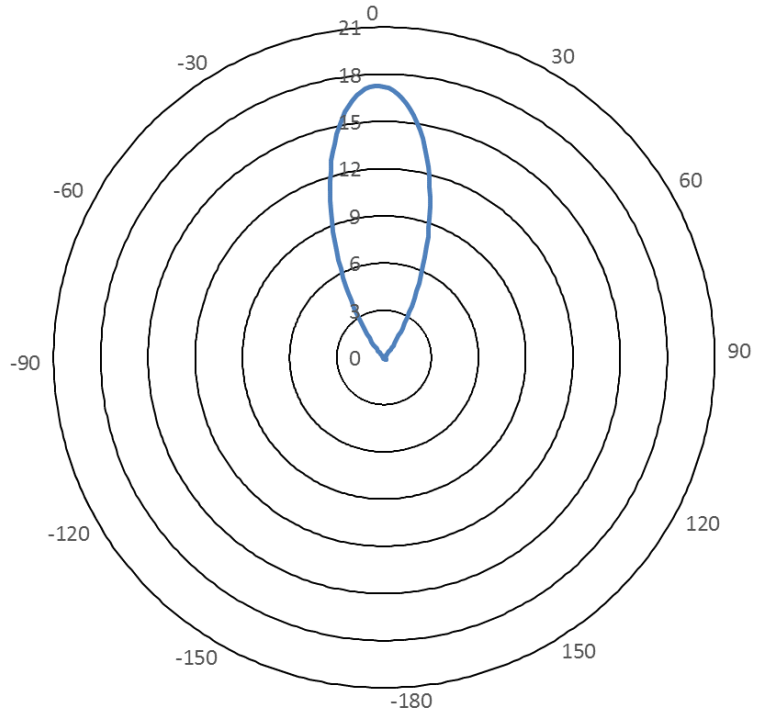

Figure 4.15 directivity of 6 elements Yagi antenna in linear scale

To compare the directivity in logarithmically scale with in linear scale, we should put them together as a whole. Figure 4.16 shows the comparison directivity of 3 elements Yagi antenna in logarithmically scale with in linear scale, and Figure 4.17 shows the comparison directivity of 6 elements Yagi antenna in logarithmically scale with in linear scale.

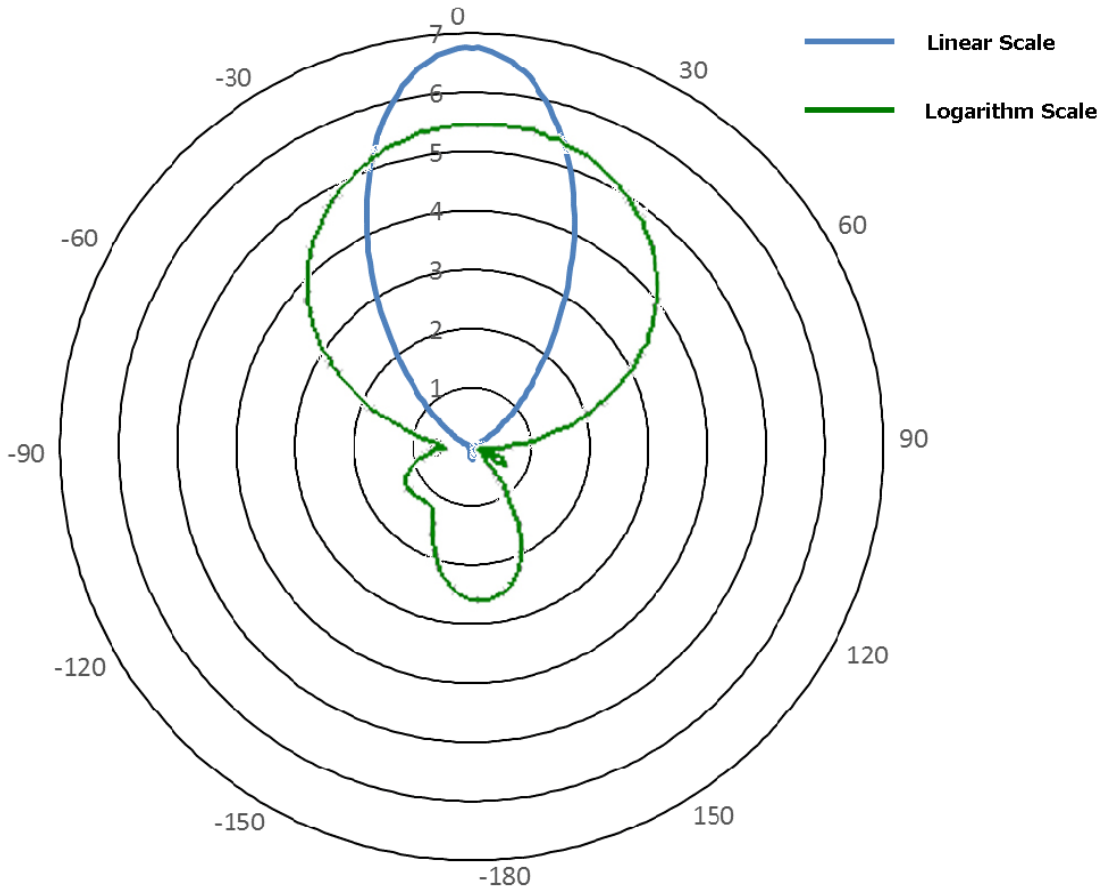

Figure 4.16 comparison the directivity of 3 elements Yagi antenna in logarithmically scale with in linear scale

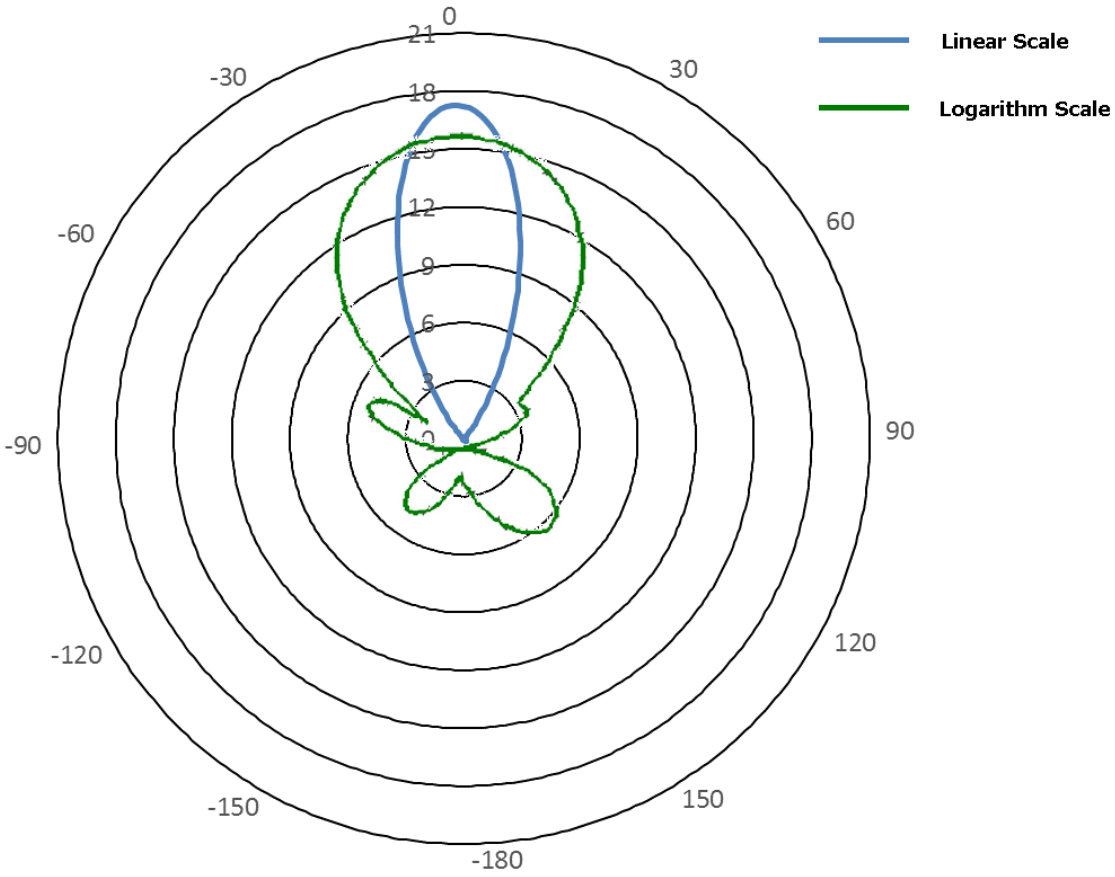

Figure 4.17 comparison the directivity of 6 elements Yagi antenna in logarithmically scale with in linear scale

4.3 Experiment

We took the data of light using camera and composed the data in one layer. In addition, we obtained five layer. At first, we introduce the directivity data of 3 elements Yagi antenna. Figure 4.18 shows number 1 layer in figure 3.3. Figure 4.19 shows number 2 layer in figure 3.3. Figure 4.20 shows number 3 layer in figure 3.3. Figure 4.21 shows number 4 layer in figure 3.3. Figure 4.22 shows number 5 layer in figure 3.3.

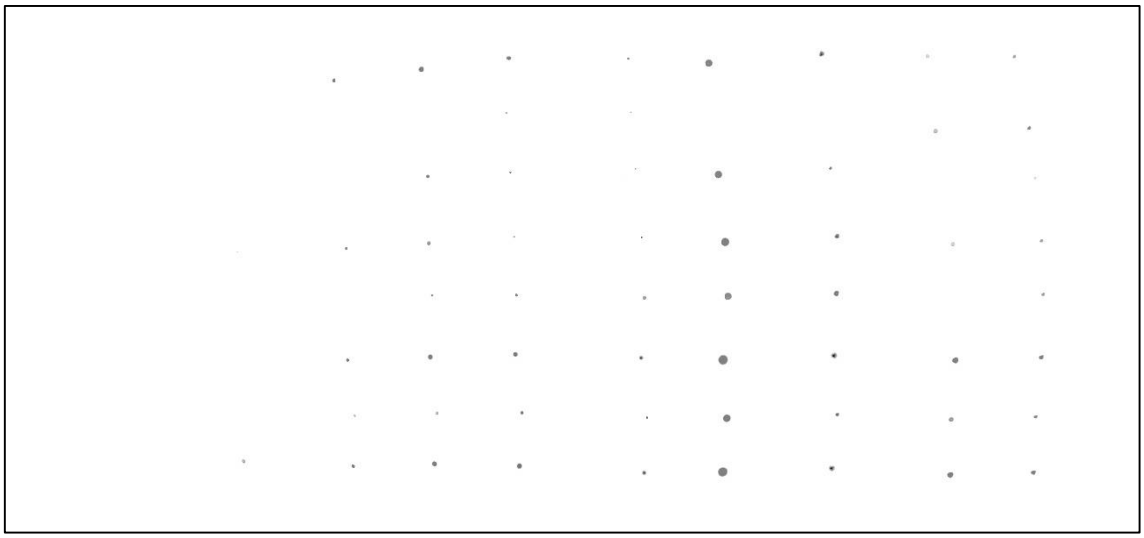

Figure 4.18 data of light of 3 elements Yagi antenna in number 1 layer

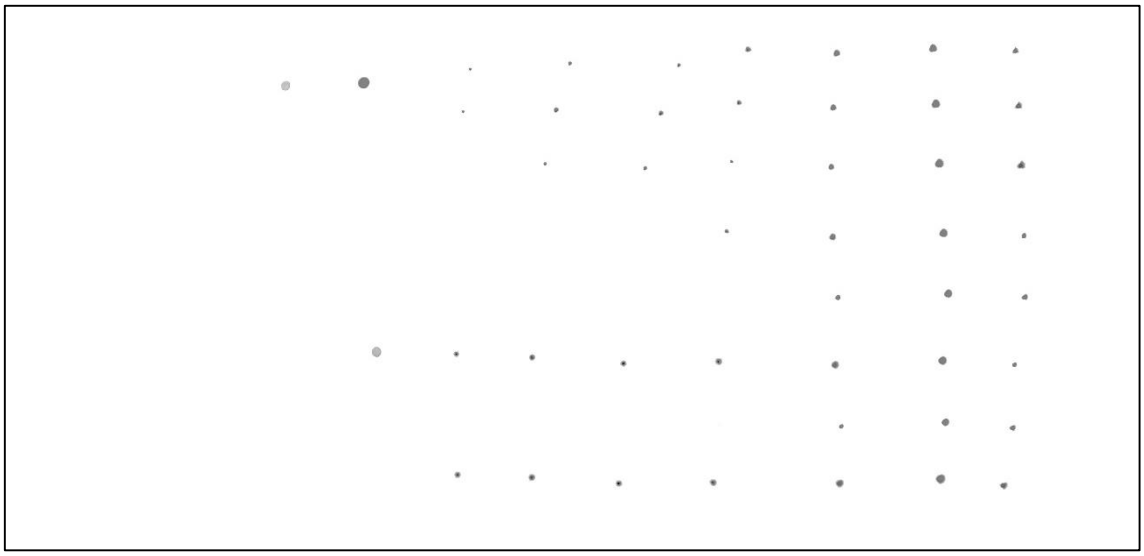

Figure 4.19 data of light of 3 elements Yagi antenna in number 2 layer

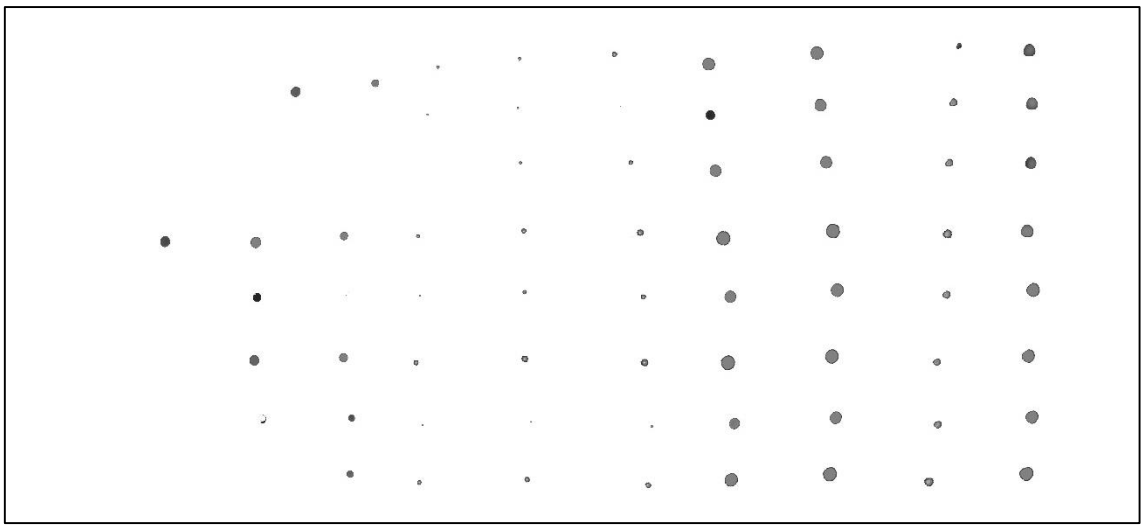

Figure 4.20 data of light of 3 elements Yagi antenna in number 3 layer

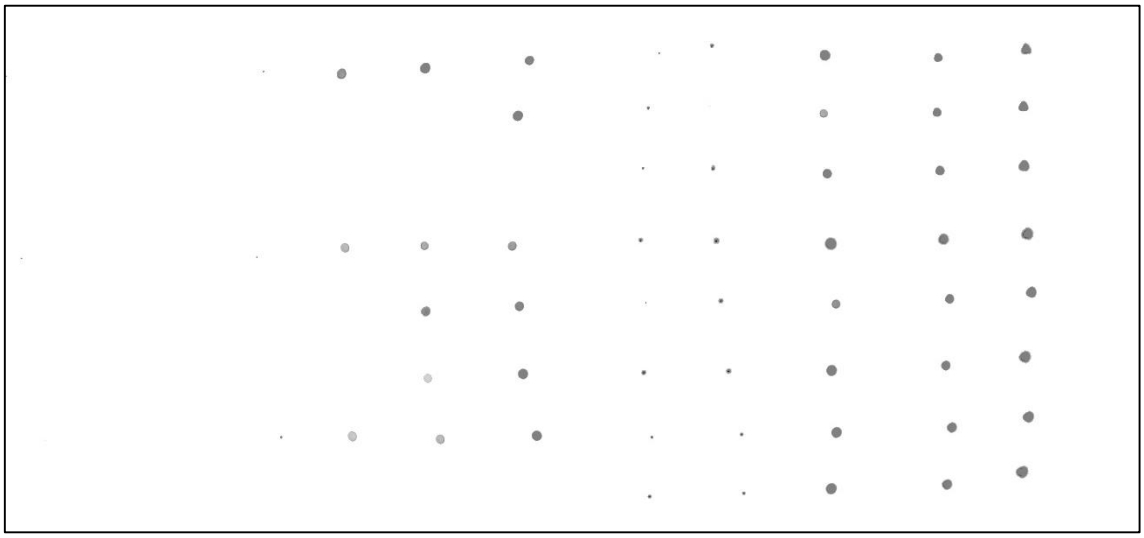

Figure 4.21 data of light of 3 elements Yagi antenna in number 4 layer

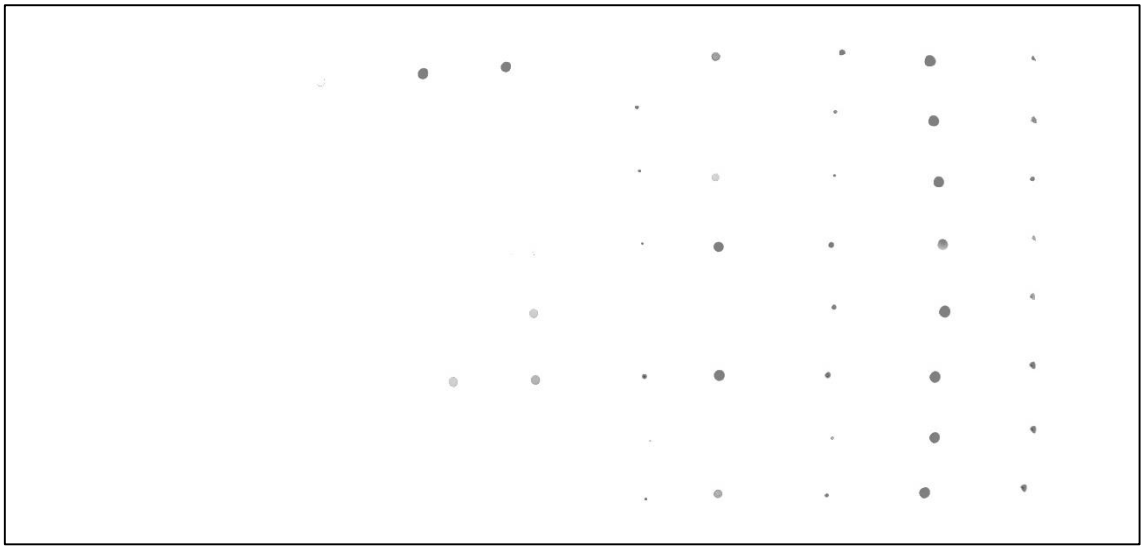

Figure 4.22 data of light of 3 elements Yagi antenna in number 5 layer

Next, we introduce the directivity data of 6 elements Yagi antenna. Figure 4.23 shows number 1 layer in figure 3.3. Figure 4.24 shows number 2 layer in figure 3.3. Figure 4.25 shows number 3 layer in figure

3.3. Figure 4.26 shows number 4 layer in figure 3.3. Figure 4.27 shows number 5 layer in figure 3.3.

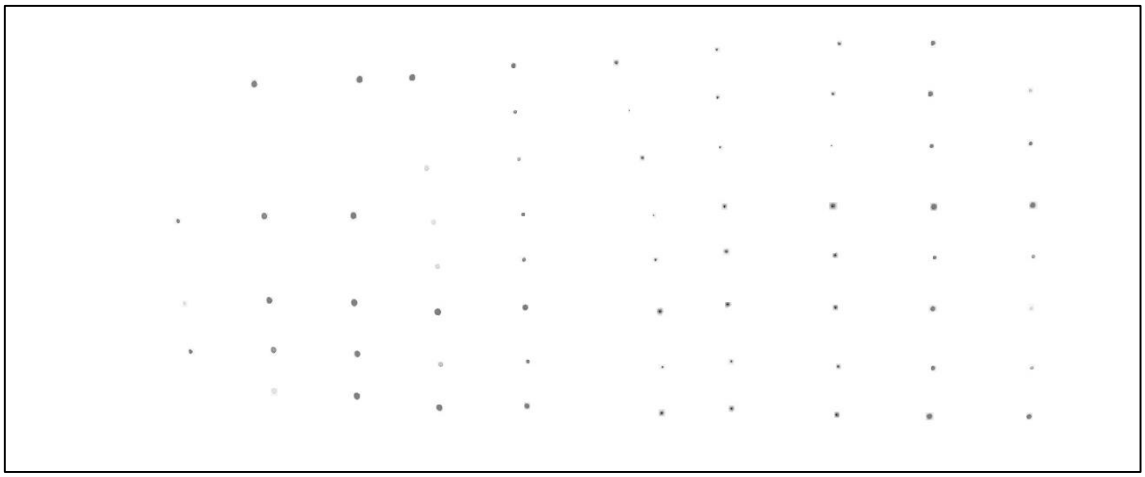

Figure 4.23 data of light of 6 elements Yagi antenna in number 1 layer

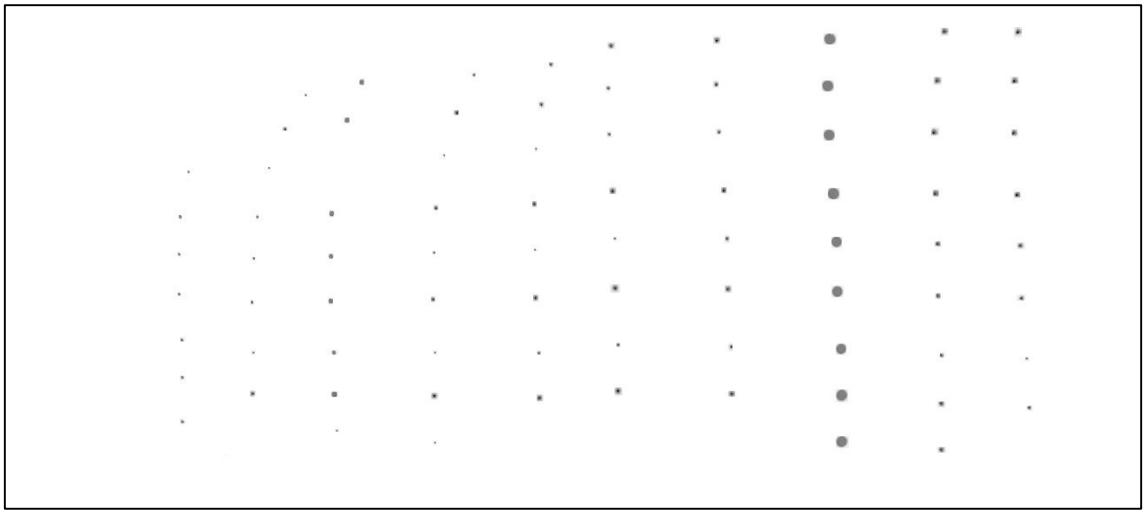

Figure 4.24 data of light of 6 elements Yagi antenna in number 2 layer

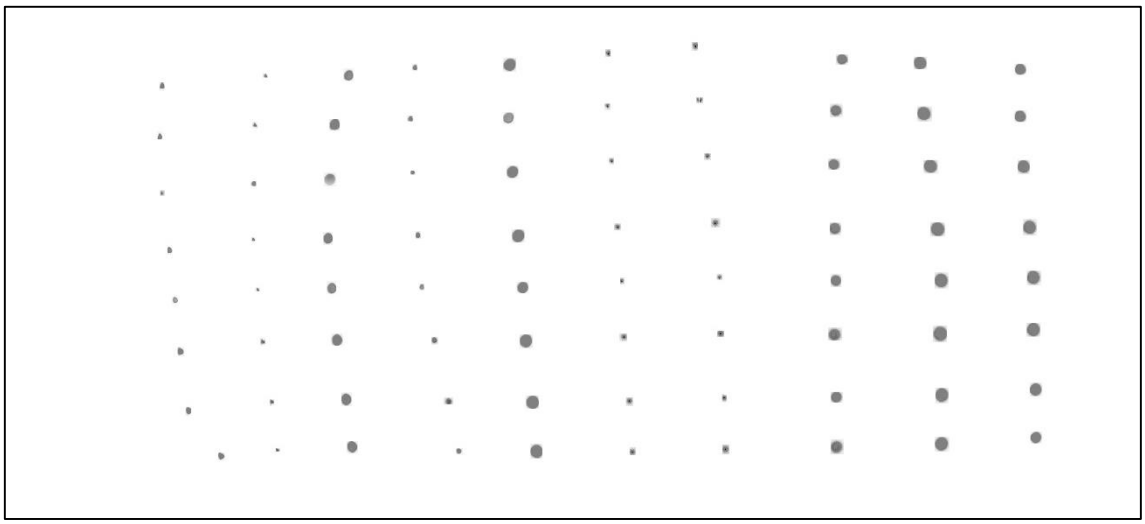

Figure 4.25 data of light of 6 elements Yagi antenna in number 3 layer

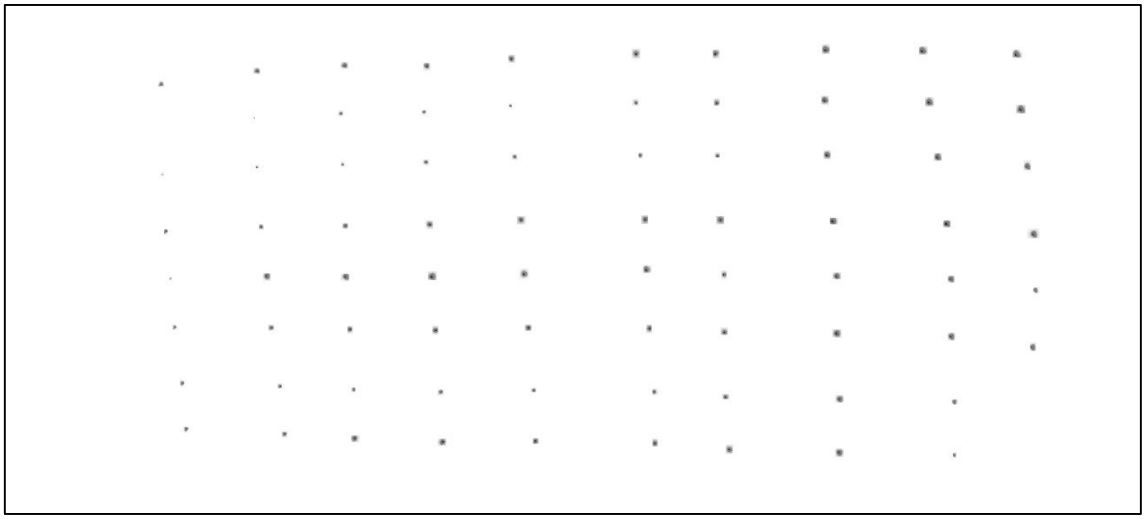

Figure 4.26 data of light of 6 elements Yagi antenna in number 4 layer

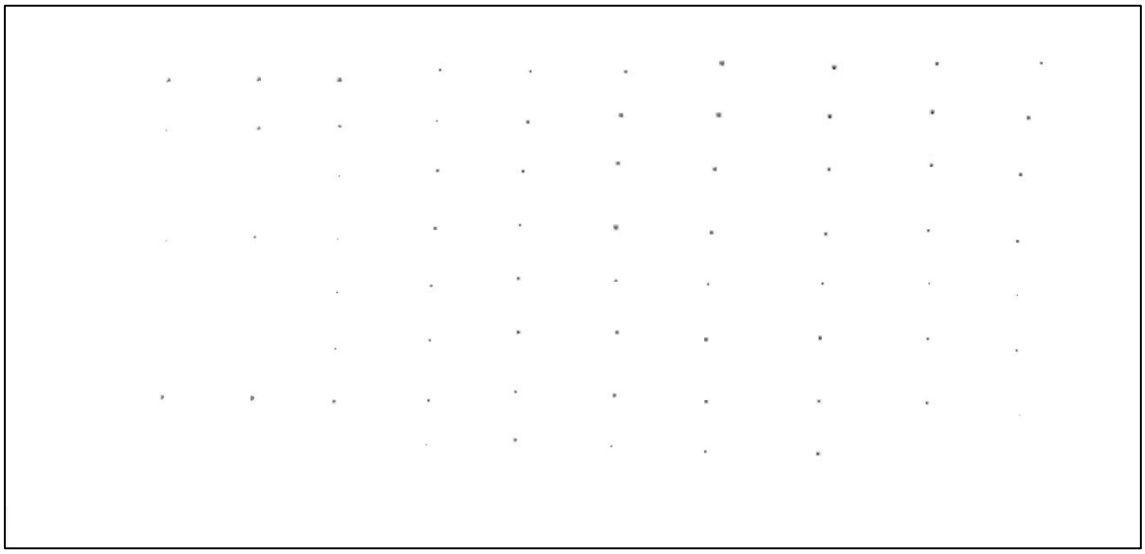

Figure 4.27 data of light of 6 elements Yagi antenna in number 5 layer

Finally, we created stereoscopic images made by combining those data using the image editing software which name is Photoshop Elements. The stereoscopic image of 3 elements Yagi antenna made by combining Figure 4.18, 4.19, 4.20, 4.21, and 4.22 is shown as Figure 4.28. The stereoscopic image of 6 elements Yagi antenna made by combining Figure 4.23, 4.24, 4.25, 4.26, and 4.27 is shown as Figure 4.29. Moreover, we combined the stereoscopic image and the directivity in linear scale to compare. The comparison of the stereoscopic data and the directivity in linear which is shown as Figure 4.14 of the 3 elements Yagi antenna is shown as Figure 4.30. In addition, the comparison of the stereoscopic image and the directivity in linear scale which is shown as Figure 4.15 of the 6 elements Yagi antenna is shown as Figure 4.31.

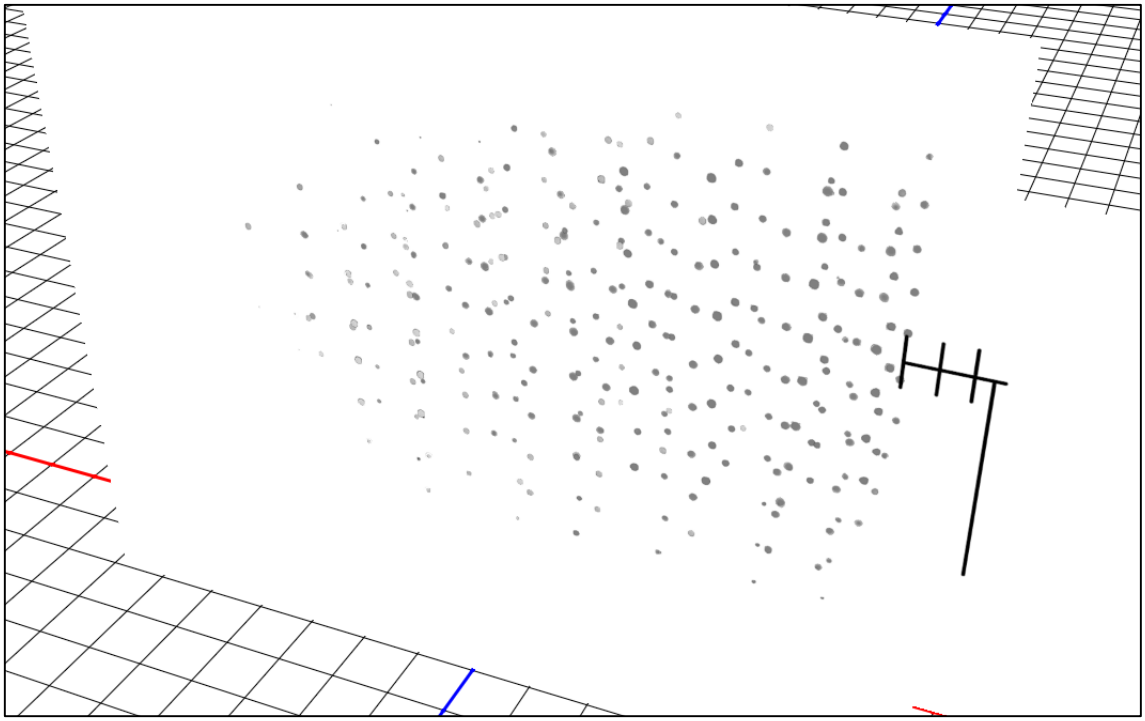

Figure 4.28 stereoscopic image data of 3 elements Yagi antenna

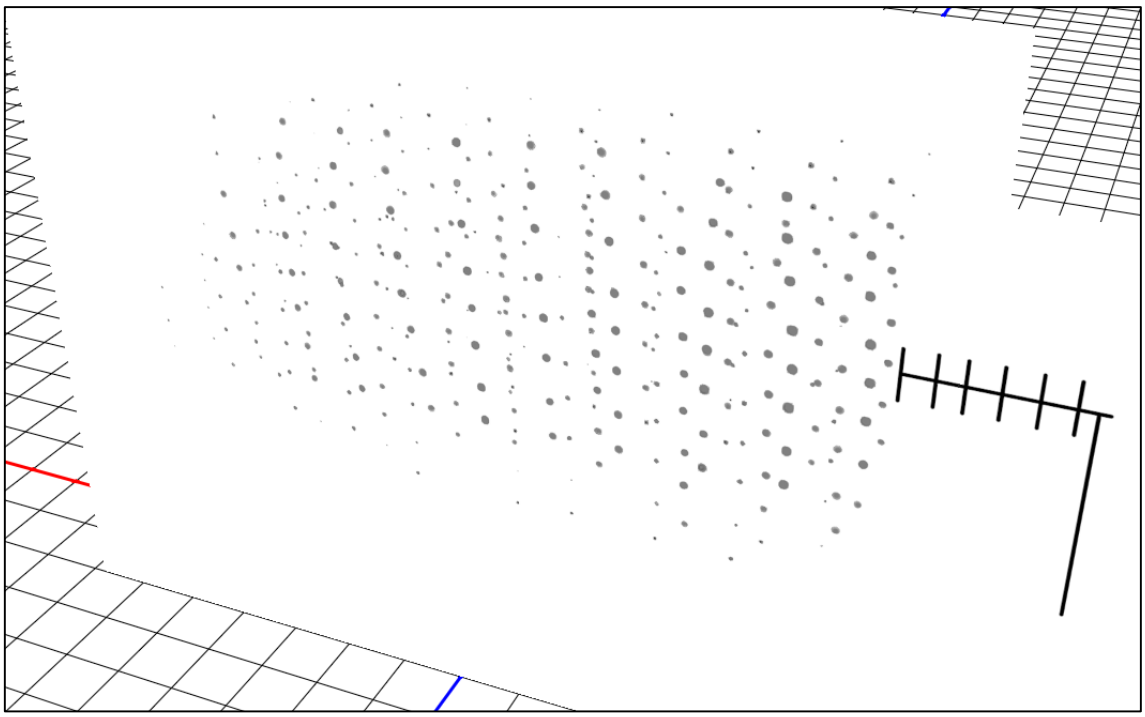

Figure 4.29 stereoscopic image data of 6 elements Yagi antenna

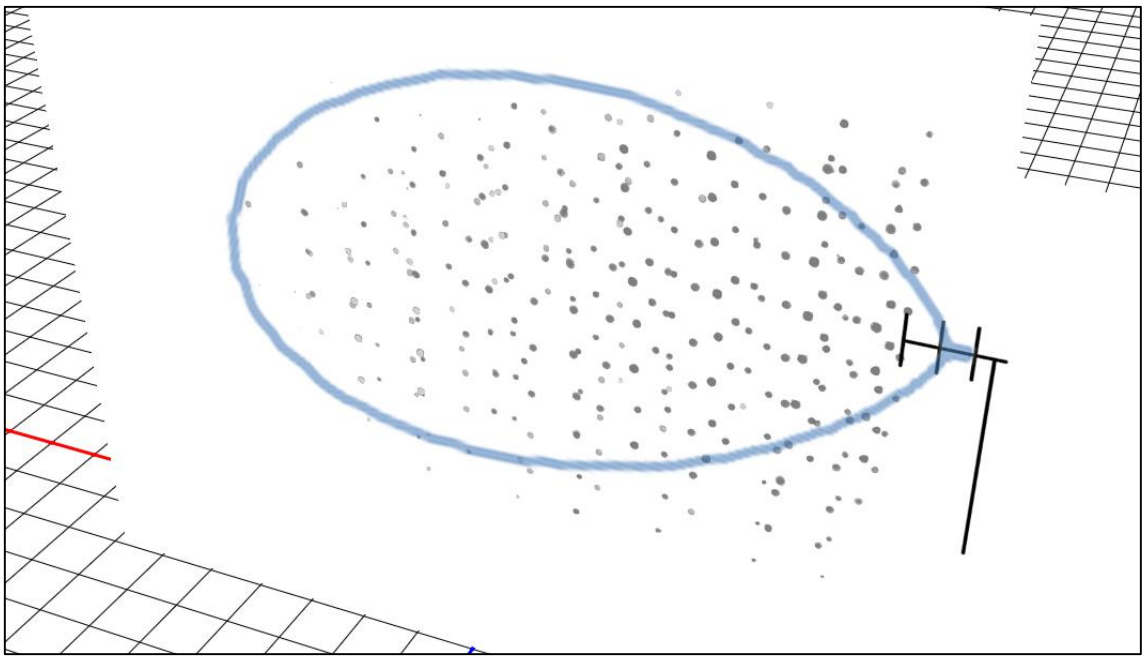

Figure 4.30 comparison of stereoscopic image and directivity in linear scale of 3 elements Yagi antenna

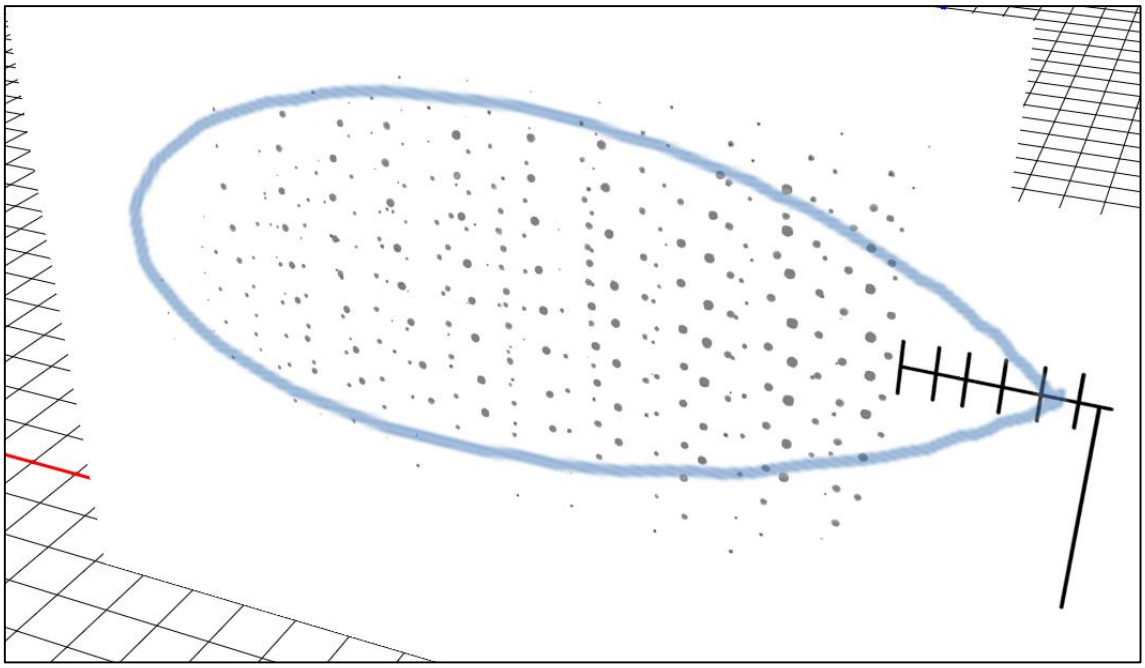

Figure 4.31 comparison of stereoscopic image and directivity in linear scale of 6 elements Yagi antenna

Chapter 5

Analysis

In this section, in order to check the precision of the visualization system, we compare the measurement data obtained in the real field with obtained in anechoic chamber.

5.1 Luminance Conversion

To check the precision of the visualization system, we have to convert the analog data obtained by camera into digital data. Method of This conversion is using image edition software (Photoshop Elements). However, this software only can get the RGB data from image. Therefore, we have to convert the RGB data into luminance data to check the precision. Luminance data is able to get by following formula [15]:

$$\begin{bmatrix} Y \\ C_B \\ C_R \end{bmatrix} = \begin{bmatrix} 0.299 & 0.587 & 0.114 \\ -0.169 & -0.331 & 0.500 \\ 0.500 & -0.419 & 0.081 \end{bmatrix} \times \begin{bmatrix} R \\ G \\ B \end{bmatrix}$$

Where Y is luminance component, C_B is blue-difference chrominance component, and C_R is red-difference chrominance component. In this case, we do not care about C_B and C_R. We need to know only Y, so we convert RGB data into Y using following formula:

$$Y = 0.299 * R + 0.587 * G + 0.114 * B$$

We calculated the luminance data of 3 elements Yagi antenna using above formula which is shown as table 5.1. In addition, we calculated the luminance data of 6 elements Yagi antenna which is shown as table 5.2.

Table 5.1 luminance data of 3 elements Yagi antenna

	Column									
Row	0	0	99	120	110	128	92	88	87	14
	0	70	99	79	88	128	128	128	62	64
	0	0	50	79	112	114	127	128	110	84
	33	40	45	66	85	100	130	127	150	100
	20	45	47	66	80	99	120	128	154	119
	0	29	33	55	80	103	136	133	110	101
	0	29	50	88	99	124	119	104	80	70
	0	40	50	70	100	80	92	74	30	26

Table 5.2 luminance data of 6 elements Yagi antenna

	Column									
Row	118	121	124	131	127	113	104	120	117	120
	105	120	127	135	130	170	132	122	125	119
	120	130	122	130	131	133	210	150	128	120
	108	111	125	128	132	134	150	203	181	128
	105	115	122	128	132	150	142	172	170	128
	100	120	121	131	133	140	180	155	122	120
	110	120	122	130	131	140	133	120	125	120
	102	118	122	135	122	119	120	150	108	106

5.2 Pearson Correlation Coefficient

In order to check the precision of the visualization system, we used the Pearson correlation coefficient. Pearson correlation coefficient is a statistical measure of the strength of relationship between paired data. In a sample it is denoted by r and is by design constrained as follows

$$-1 \leq r \leq 1$$

Furthermore, positive values denote positive correlation, negative values denote negative correlation, a value of 0 denotes no correlation, and the closer value is to 1 or -1, the stronger correlation. Moreover, correlation is an effect size and so we can verbally describe the strength of the correlation using the guide that Evans (1996) suggests for the absolute value of r [16]:

- .00-.19 “very weak”
- .20-.39 “weak”
- .40-.59 “moderate”
- .60-.79 “strong”
- .80-1.0 “very strong”

Moreover, Pearson correlation coefficient r is defined as following formula [17]:

$$r = \frac{\frac{1}{N}\sum_{i=1}^{N}(X_i - \bar{X})\,(Y_i - \bar{Y})}{\sqrt{\frac{1}{N}\sum_{i=1}^{N}(X_i - \bar{X})^2}\sqrt{\frac{1}{N}\sum_{i=1}^{N}(Y_i - \bar{Y})^2}}$$

Where r is pearson coefficient, N is number of data, X_i *and* Y_i is dataset; $\{x_1, \dots, x_n\}\{y_1, \dots, y_n\}$. We calculated Pearson correlation coefficient per rows. From the top, we defined row names as r1, r2, r3, r4, r5, r6, r7, and r8. Table 5.3 shows the Pearson correlation coefficients of 3 elements Yagi antenna and 6 Yagi antenna per rows.

Table 5.3 Pearson correlation coefficients of 3 element and 6 elements Yagi antennas.

	elements	
	3	6
r1	0.586	0.590
r2	0.735	0.481
r3	0.726	0.632
r4	0.798	0.904
r5	0.750	0.907
r6	0.645	0.721
r7	0.515	0.450
r8	0.234	0.648
Ave.	0.624	0.667

We are able to confirm that 3 elements Yagi antenna is strong positive correlation and 6 elements Yagi antenna is also strong positive

correlation according to calculated r and Evans suggestions. Near the center, Pearson correlation coefficient is high value both 3 elements and 6 elements Yagi antennas. However, Pearson correlation coefficient is low toward the outer side. Furthermore, lower part is lower correlation than higher part. It is thought that reason of those differences between Pearson correlation coefficient of higher part and lower part is reflection by the ground.

Chapter 6
Conclusion

6.1 Conclusion

We are able to illustrate the directivity of the antenna if we use the anechoic chamber. However, it is so difficult for us to illustrate the directivity of the antenna in the real fields. Therefore, we proposed and assembled the system that aim to be able to visualize the directivity of antennas in the real fields. In this experiment, we accomplished to assemble the visualization system and to visualize the directivity of antennas. View of experiment results, we confirmed the difference between Yagi antennas which has 3 elements and 6 elements. Comparing the experiment results and the simulation results using pearson correlation coefficient, average value is 0.62 (3 elements) and 0.67 (6 elements). Those values mean moderate match. The precision of the visualization system does not reach perfection. However, experiment results are close data with simulation one.

6.2 Future work

The visualization system does not reach perfection. So we aim to improve the system and carry out more experiment in other situations.

Appendix

Unmanned Aerial Vehicle based Missing People Detection System employing Phased Array Antenna

Published in : Wireless Communications and Networking Conference Workshops (WCNCW), 2016, IEEE

- **Abstract**

In this paper, we propose a system for detection of the missing people employing UAV which is able to move quickly and has a wide view from the air in the disaster area. However, an airplane type UAV does not always have a stable flight due to strong wind, rolling, and pitching. In order to detect and to respond the missing people promptly using the UAV, we propose the system which uses a phased array antenna and an angle detector. To implement the system, we assemble the phased array antenna and carry out an experiment to measure the characteristics of directivity, the directivity control characteristics, the return loss of the antenna, and the received power level to compare using and not using the phased array antenna in terms of efficiency and functionality. The experiment results show that the proposed system increase the received power level by adjusting the directivity of the antennas with short delay time. The results also confirm that the proposed system is practical in decreasing victims of disasters.

● INTRODUCTION

In recent years, it has been raised in importance about UAV which stands for Unmanned Aerial Vehicle or Unmanned Automobile Vehicle and originally the UAV has been used by the military [1] [2]. For example, the UAV has been used as a reconnaissance plane which name is a Global Hawk in America. However, recently, the UAV has been utilized in a broad range of fields and caught a great attention in research field. And in this paper, we focused on utility of the UAV when it happened the disaster.

In 2011, The Great East Japan Earthquake occurred. This disaster caused serious damages. The number of suffers from it are 24635. To reduce the victims, we are required to detect missing people as soon as possible [3] [4]. However, we could not detect the missing people quickly on the ground because some roads collapsed due to terrible earthquake or tsunami and the radioactivity leaked out of the nuclear power plant. There is the limitation to detect them on the ground.

In contrast, the UAV moves in the air and investigate something quickly and the UAV can go and search the place people hardly to go. Moreover, the UAV can investigate the environment and the UAV is applied supervisory system. An application examples of monitoring or supervisory system employing the UAV are that observe a landslide and a road condition after serious disaster which is like earthquake and a condition of forest fire and that rescue and that measure a leaked radiation dosage from a nuclear power plant. In fact, some UAVs were

used when The Great East Japan Earthquake occurred. That is why the UAV is cut out for it and the UAV attracted attention all over the world. Thus, studies on the UAV will increase. However, the UAV which is like a plane has a problem. When this type of the UAV is equipped with an antenna or antennas rocks due to heavy wind, those antennas swing with the movement of the UAV.

In this paper, we focus on the system for disaster and propose the system which searches missing people in the disaster area using UAV with some sensing technologies [5]. In the future, when serious disaster may happen and cause a large number of missing people, we can suggest the system using UAV for detecting missing people in the disaster area.

In our proposed system, users of the system should wear the transponder which is like a wristwatch and able to transmit and receive a signal. And the transponder receives the signal from the UAV and then sends an identification signal or a binary data to the UAV. As for the missing people detection, an ideal antenna to use covers a wide range and reaches a long area. However, a wide directional antenna like a patch antenna is low gain and does not get enough field intensity. A high gain antenna has a sharp directivity in contrast with like a patch antenna, and has a problem which is hard to get enough field intensity due to direction for the antenna. If we choose the patch antenna for system, though this antenna has a relatively wide directivity, a beam from the antenna will not reach that far. On the contrary, if we choose

the high gain antenna, though a beam will reach relatively far, this antenna will not point wide area due to have a sharp directivity. Each antenna has some demerits and is not effective for detecting missing people. As a solution to the problem, we should consider to change detection of the beam.

We are able to conceive some methods to change detection of the beam as follows.

- an antenna attached to the UAV moves physically. This method uses an angle detector and a motor. The angle detector calculates the tilt angle of the UAV and the motor moves the antenna.
- A beam from the antenna moves and antenna does not move. This method uses an angle detector and phased array antenna [6] [7]. Phased array antenna has several antennas and controls a phase of each elements and adaptively controls for the directivity.

To determine which between the two methods is effective, we carried out the experiment which flew the UAV and recode the flight altitude tilt angle of the UAV. Using the UAV is illustrated in Fig. 1. And we obtained the data from this experiment. Fig. 2 shows the relationship between rolling angle and passed time, Fig. 3 shows the relationship between pitching angle and passed time.

From the initial results, we can consider that the second method which uses the phased array antenna is a better way to solve that problem because those figures show that each angles change very quickly. Thus,

we consider that the method which moves physically is not an appropriate way to solve the problem.

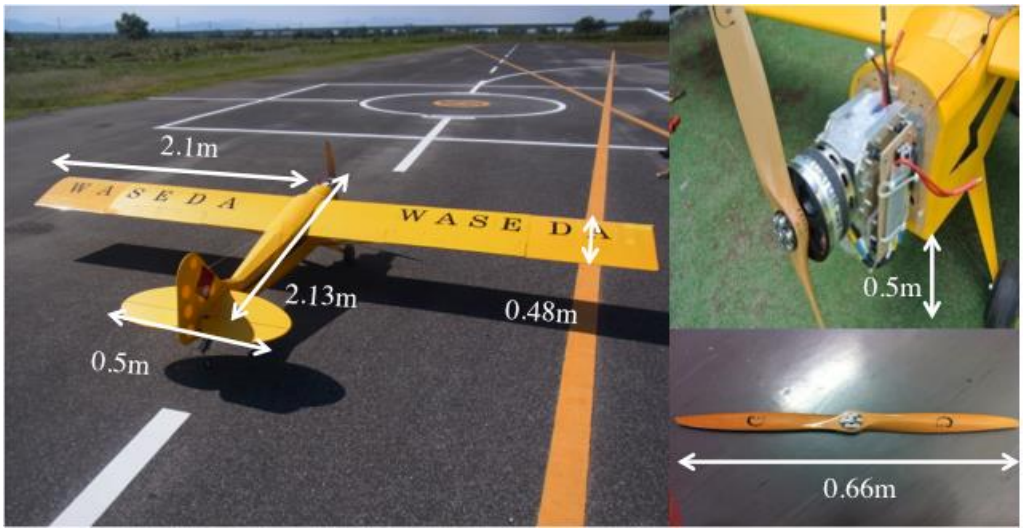

Figure 1 UAV used in the flight experiment

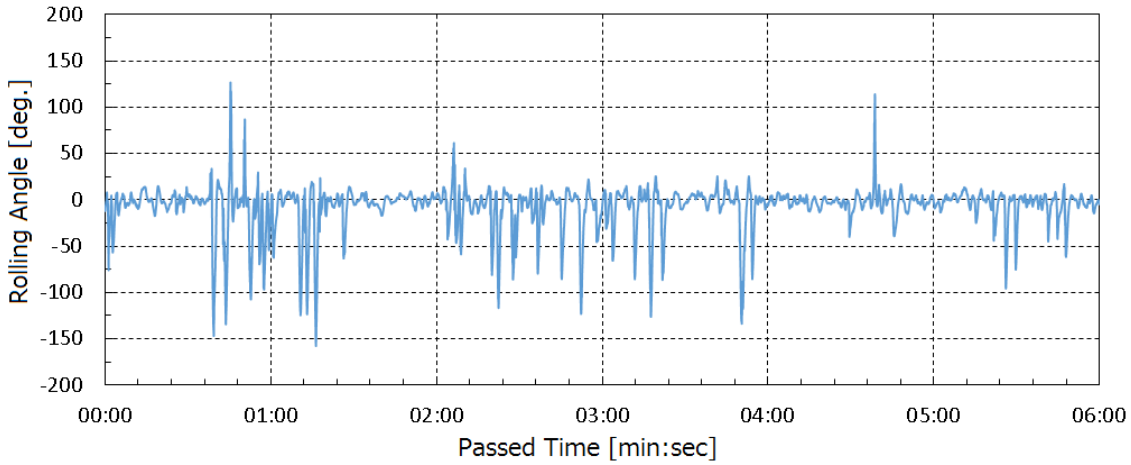

Figure 2 relationship between rolling angle and passed time

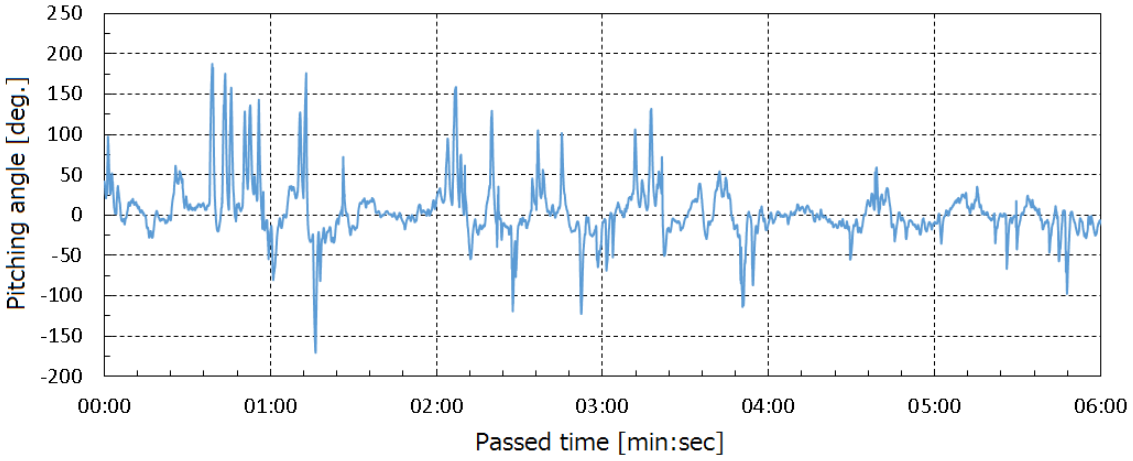

Figure 3 relationship between pitching angle and passed time

● SYSTEM MODEL

In order to solve the problem that the beam of an antenna or antennas moves with movement of the UAV, our proposed the system uses a phased array antenna. The conventional system has to move through a wide area because of low antenna gain and the beam from the antenna points downwards as shown in Fig. 4. Unlike the conventional system, our proposed system also steers directivity of the antenna which has a high gain when the flight is stable as shown in Fig. 5.

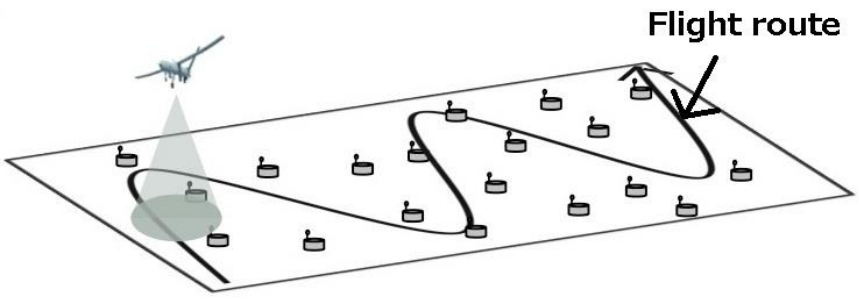

Figure 4 Flight route using the conventional system

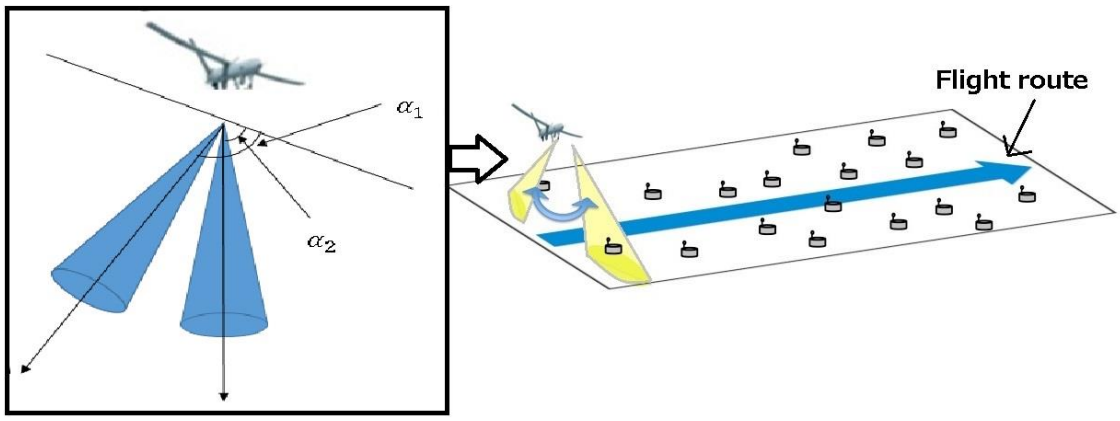

Figure 5 Flight route using the proposed system

A. Conventional System

The conventional system just has a fixed patch antenna, which directivity is wide and gain is not high, below the UAV. When the UAV detects people, there is a problem that a beam from an antenna swings when the UAV pitches, rolls, and has a bumpy flight due to bad weather such as strong wind or heavy rain. In addition, if the UAV flight is stable, the beam from the antenna only directs downwards and thus this conventional system has to move windingly as illustrated in Fig. 4. This system is not efficient, considering the battery capacity [8].

B. Proposed System

On the other hand, in our proposed system, since we use the angle detector, this system is able to more effectively detect the missing people when the UAV is not stable flight. For using this system, we are able to always detect a beam in the same direction using the angle detector which is able to detect the tilt angle of the UAV in real time. Moreover, this system maintains the angle of the beam using the

information from the angle detector and steers the antenna directivity using the phased array antenna.

C. Antenna

In order to construct the proposed system, we consider an antenna which is the kernel of the system. We need an antenna that has a high gain and can search through wide areas.

1) Array antenna: An array antenna has a high gain and can steer the directivity thus it can search through a large surface. An array antenna is constituted of some antenna elements arranged regularly and a feeder circuit to radiate and excite from the antennas and as shown in Fig. 6. The type of antenna which is used an array antenna is a wire antenna which is like a dipole antenna or a antenna which has a beam having a comparatively low gain and a wide beam like a micro strip antenna or a slot antenna. As for the feeder circuit, there are various kinds. Not only constituted of a distribution or synthetic circuit but a phase shifter, a high output amplifier, and a low noise amplifier. In an array antenna, various functions of antenna which individual antenna could not realize are materialized by of changing the type of antenna, arrangement method, and excitation method of element antennas.

The signals from the antennas are combined in order to get a high gain over that of a single antenna. Features of the array antenna which individual one could not gain are high gain due to increase of element antennas and side lobe suppression due to arrangement of element antennas.

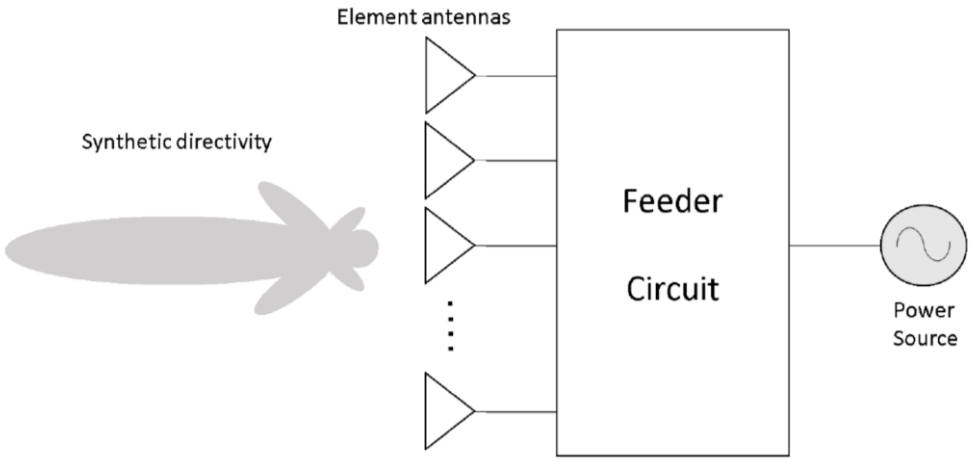

Figure 6 Constitution of an array antenna

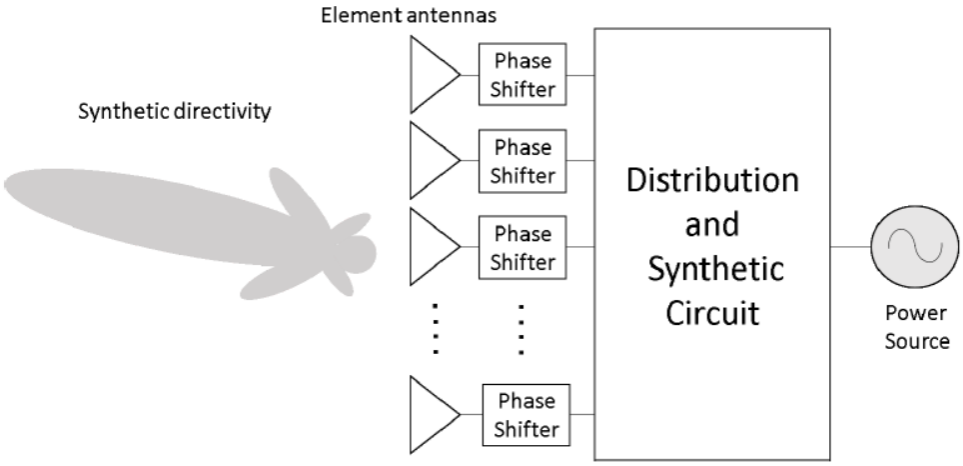

Figure 7 Constitution of a phased array antenna

Moreover, an array antenna is able to steer the directivity. This type of array antenna is named beam scanning antenna on account of beam scanning. This type of antenna can point a main lobe of antenna at aiming direction and one of these is named the phased array antenna.

2) Phased array antenna: A phased array antenna is one of array antennas, composing with lots of radiating elements with a phase

shifter as shown in Fig. 7. Beams are synthesized by shifting the phase of the signal emitted from each radiating element so as to steer the beams in the desired direction. Each element adjusts excitation phase by a phase shifter and phases become equal in the θ direction because of directing the beam of the phased array antenna in the θ direction. In this way, the phased array antenna can steer the beam of antenna electronically by adjusting the excitation phase. We assembled a phased array antenna and a linear antenna with a purpose to assemble a more effective antenna than patch antenna. Number of elements of an assembled phased array antenna is 4 and of an assembled linear array antenna is 4 and 8.

Below, there is description of assembling. A phased array antenna arrays parallel to N element antennas interval d to Xaxis as shown in Fig. 8. If directional radiation patterns of each element are on the same axis, directional radiation of an array antenna can be improved considering only phase difference from arrangement of elements [9] [10]. In Fig. 8, a position vector of n-th element is shown as

$$\boldsymbol{r_n} = (x_n, 0, 0) \qquad (1)$$

A excitation amplitude is an, an excitation phase is n, and a directivity of element is $g(\theta, \varphi)$ using the angle of the polar coordinates expressed by (θ, φ). Furthermore, a direction vector of the observation point is expressed as follows [9]:

$$\boldsymbol{R} = (\sin\theta\cos\varphi\,,\sin\theta\sin\varphi\,,\cos\theta) \tag{2}$$

Radiation directivity of the linear array antenna in Fig. 8 is expressed by following formula [9].

$$E(\theta,\varphi) = g(\theta,\varphi)\sum_{n=0}^{N-1} a_n e^{j\varphi_n}\, e^{jk_0 \boldsymbol{r_n}\cdot\boldsymbol{R}} \tag{3}$$

$$= g(\theta,\varphi)\sum_{n=0}^{N-1} a_n e^{j\varphi_n}\, e^{jk_0 nd\sin\theta} \tag{4}$$

Where k_0 is $2\pi/\lambda$. Meaning of k_0 is wave number in freespace and λ is free-space wavelength.

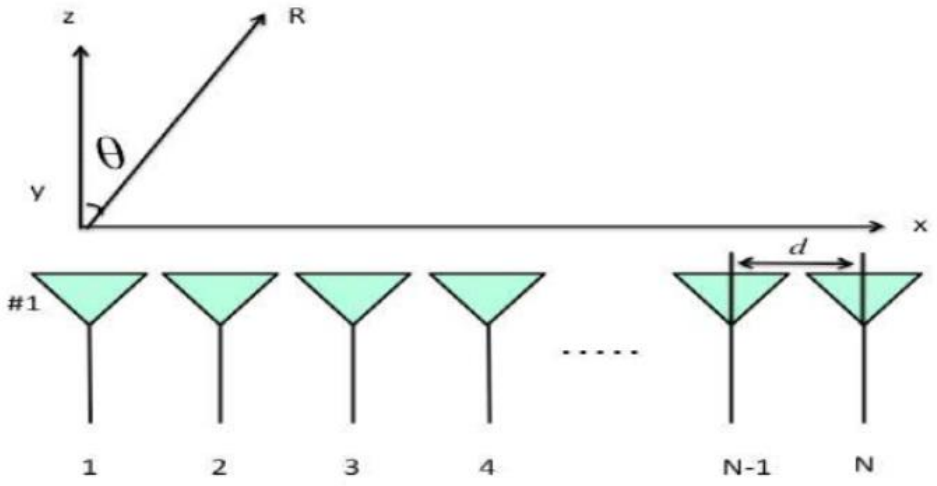

Figure 8 Constitution of a linear array antenna

● EXPERIMENT SET UP

For the construction of the proposed system, we measured the various characteristics of the antenna which is the kernel of the system. The measuring characteristics were the characteristics of directivity, the control directivity characteristics, the characteristics of the return loss when using antenna, and received power level of the communication distance.

A. Experiment of phased array antenna

We assembled a phased array antenna which is shown in Fig. 9 for construction of the proposed system and a phased array antenna had lots of phase shifters to steer the direction of the beam. Thus, we needed to know how voltage changes the value of phase shift. For assembling the phased array antenna, we measured the phase control characteristics of the 8 phase shifters using the network analyzer. Then we measured the phase control characteristics of the combination of two phase shifters. The maximum of the UAV beam's angle which can be changed was 30 degrees using our equipment. In order to obtain the desired angle of the UAV beam, it was necessary to decide the shift angle of the shifters. The parameters of the shifters with different combinations are shown in table I. Here, α is the angle between the UAV and the beam direction which is shown in Fig. 5, where $\alpha = \theta + 90$.

Moreover, we measured the directivity for the assembling phased array antenna which was composed of 4 elements and the difference of

the directivity between 1 element, 4 elements, and 8 elements in the anechoic chamber.

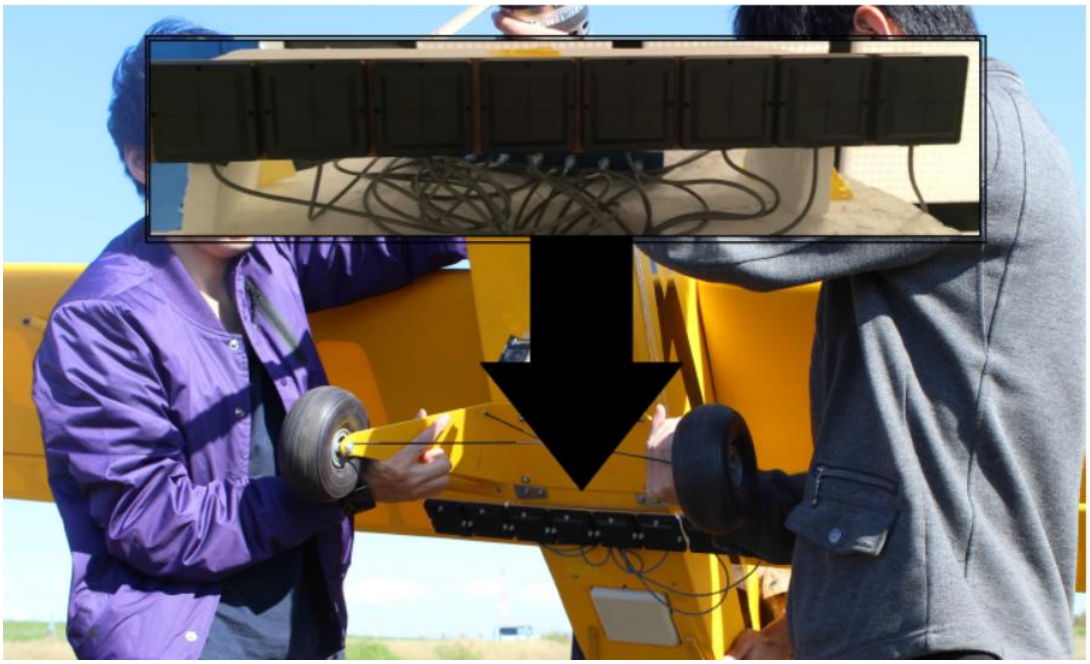

Figure 9 Loading phased array antenna on UAV

TABLE I Required phase difference to steer directivity

α [deg.]	$\cos\alpha$	N=1	N=2	N=3	N=4
60	0.5	0	90	180	270
70	0.34	0	61.56	123.12	184.69
80	0.17	0	31.26	62.51	93.77
90(front)	0	0	0	0	0
100	-0.17	0	-31.26	-62.51	-93.77
110	-0.34	0	-61.56	-123.12	-184.69
120	-0.5	0	-90	-180	-270

B. Experiment of measurement of the return loss of antennas

We measured the return loss value of each antennas because this value indicates the performance of an antenna. Where return loss expresses the ratio of reflected power to the input power in dB format. Return loss value has a connection with VSWR, which stands for Voltage Standing Wave Ratio. VSWR is the ratio of the maximum voltage in standing wave pattern and the connection between return loss and VSWR.

C. Measurement experiment of the received power

We measured received power level to the communication distance of 2.4 GHz transmitter on the ground, expecting the flight communication experiment which uses the UAV. This experiment purpose was to confirm how much the received power is attenuated to the communication distance from which free space can be considered. Output power of transmitter is 250 mW and frequency is 2.458 GHz. A used antenna was a patch antenna or 4 elements phased array antenna or 8 elements phased array antenna. Transmitter moved from 0 m to 50 m while the receiver was fixed, and then we measured the distance in which transmitter and receiver are able to communicate and the received power.

● RESULT

A. Result of phased array antenna

Fig. 10 shows the phase control characteristics of the 8 phase shifters using the network analyzer. As you can see from this figure, we can confirm the phase control characteristics of the 8 phase shifters though those phase shifters have some dispersion. Moreover, as you can see from Fig. 11 and Table I, we can confirm all of combination of the phase shifters are over 360 degree and the all of combination phase shifters can accommodate the needed amount of phase shifts.

Fig. 12 shows the directivity of each array antennas which are composed of 1 element, 4 elements, and 8 elements. The green line indicates the directivity of 1 element, the red line indicates 4 elements, and the blue line indicates 8 elements. As you can see from this figure, as the number of elements increases, the directivity becomes sharper. The half-value angle of 1 element is ± 60 degrees, the value of 4 elements is ± 15 degrees, and 8 elements is ± 8 degrees.

Fig. 13 shows the directivity of the phased array antenna and Table II indicates control voltages to steer the directivity of phased array by calculating form the phase control characteristics and Table I. As you are able to see from this figure, we are able to confirm that we theoretically steer, without disturbance, the directivity.

TABLE II Control voltages

Color in Fig. 10	Control voltages			
	N=1	N=2	N=3	N=4
Green	13.5	9.0	4.5	0
Red	7.5	5.0	2.5	0
Blue	2.1	1.4	0.7	0
Pink	0	0	0	0
Gray	0	0.7	1.4	2.1
Brown	0	2.5	5.0	7.5
Purple	0	4.5	9.0	13.5

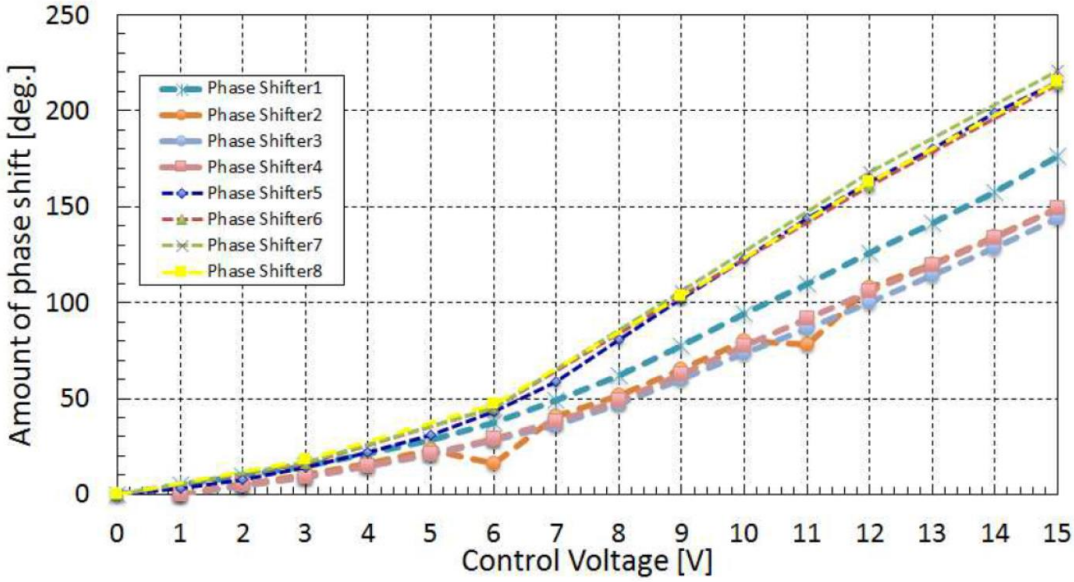

Figure 10 Relationship between control voltage and the degree of phase shift using different phase shifter

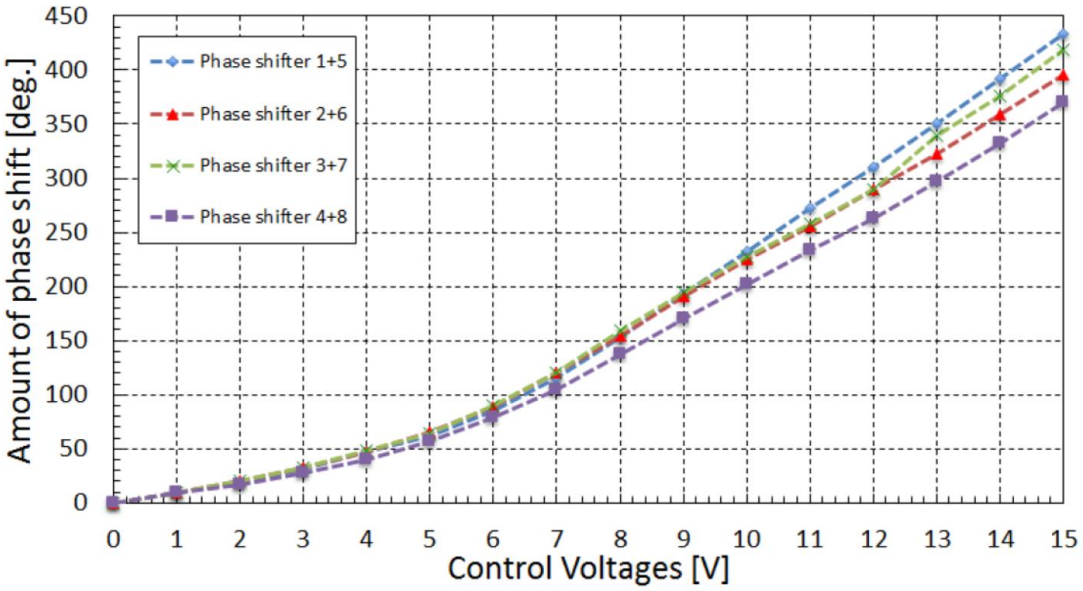

Figure 11 Relationship between control voltages and combined the degree of the phase shift using multiple phase shifter

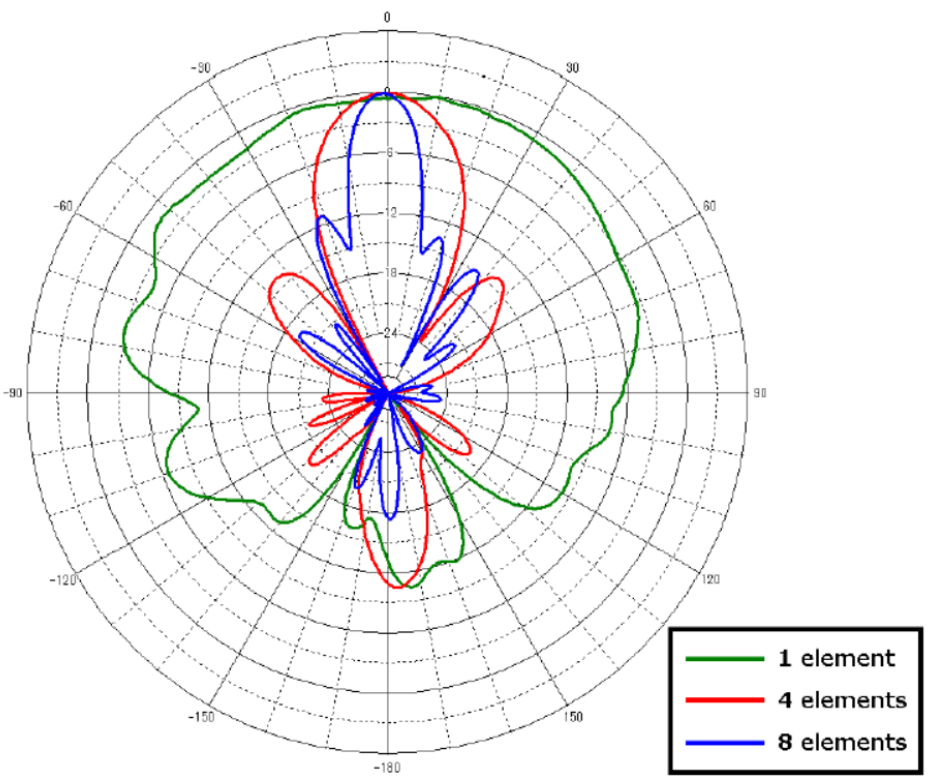

Figure 12 Directivity based on different elements composition

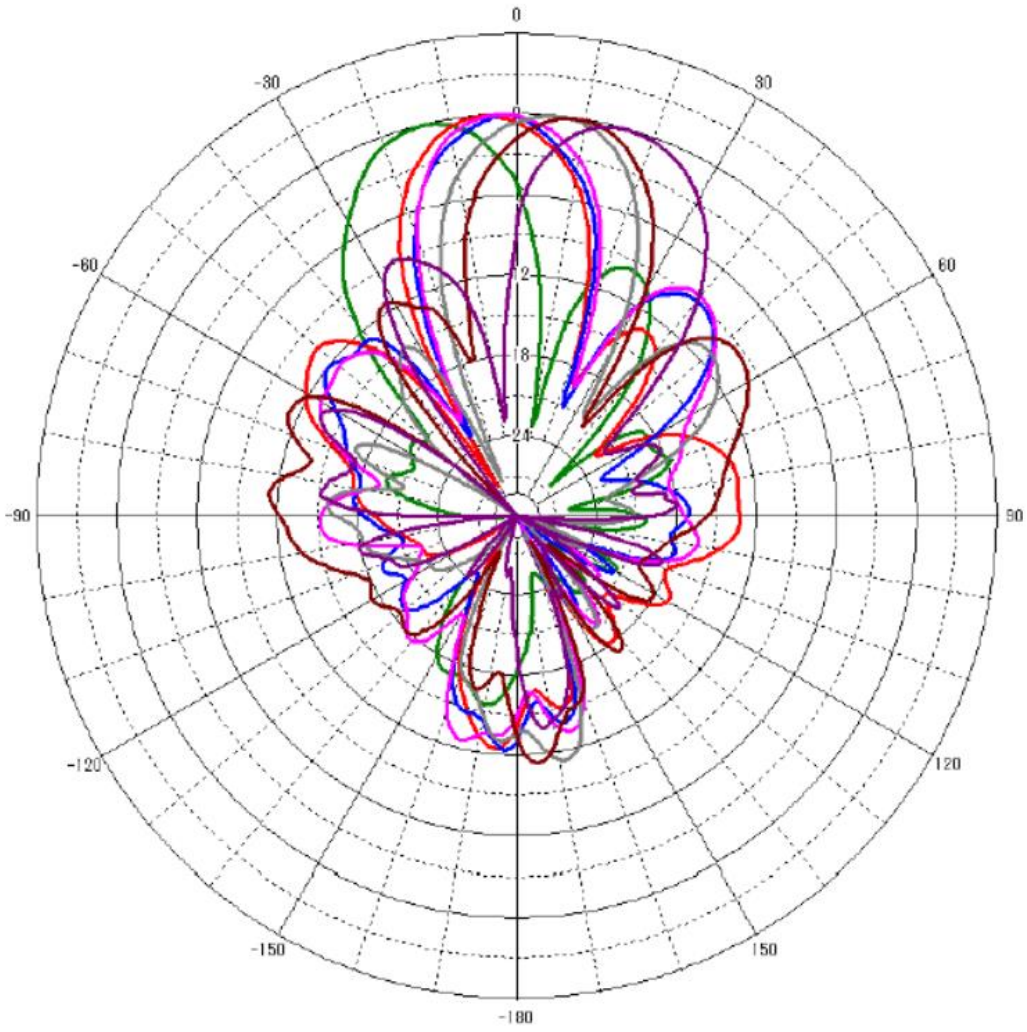

Figure 13 Directivity based on different phase shift

B. Experiment results of the return loss using antennas

The characteristics of return loss of making the phased array antenna are shown in Fig. 14. For comparing difference, we measured the characteristics of return loss each antennas. The return loss value of each antennas is below -15 dB at 2.45 GHz and the loss power is less than 0.15 dB. And we can confirm that 4 elements and 8 elements

antennas divide the signal from a transmitter adequately to each elements.

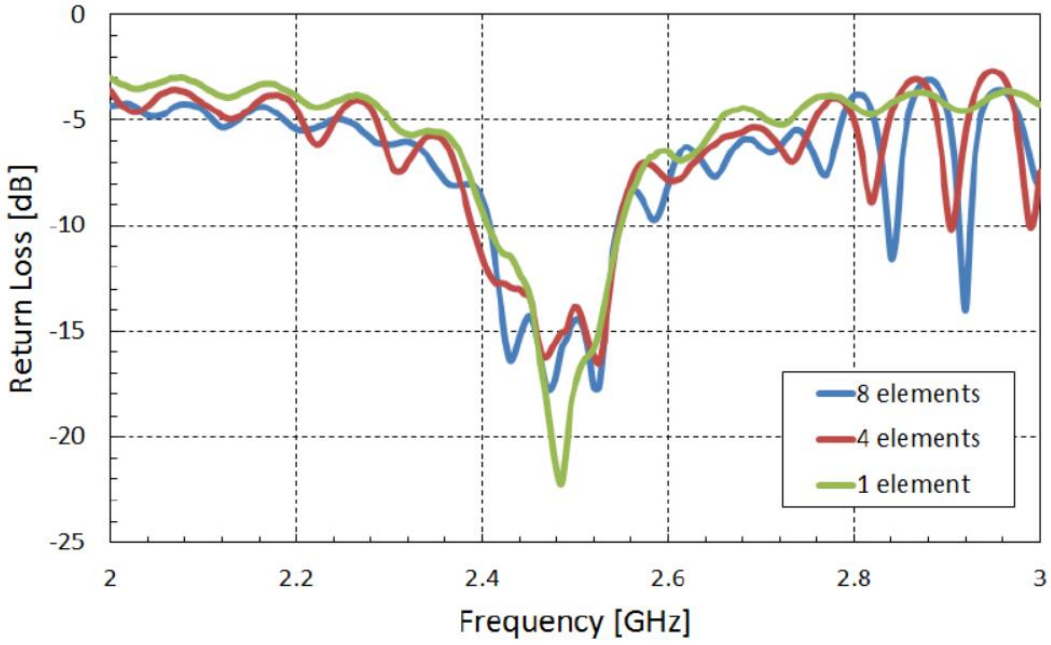

Figure 14 Return loss value of the antennas with different elements composition

C. Experiment results of the received power

Fig. 15 shows received power level of the communication distance of 2.4 GHz transmitter on the ground. As you can see from the result, 8 elements have the highest level of received power, 4 elements has middle, and 1 element has lowest at 50 m point. From this result, we found that received power increases with the number of elements. The order between 1 element and 4 elements is changed at 10 m and 30 m points, and 1 element level is a little bit high.

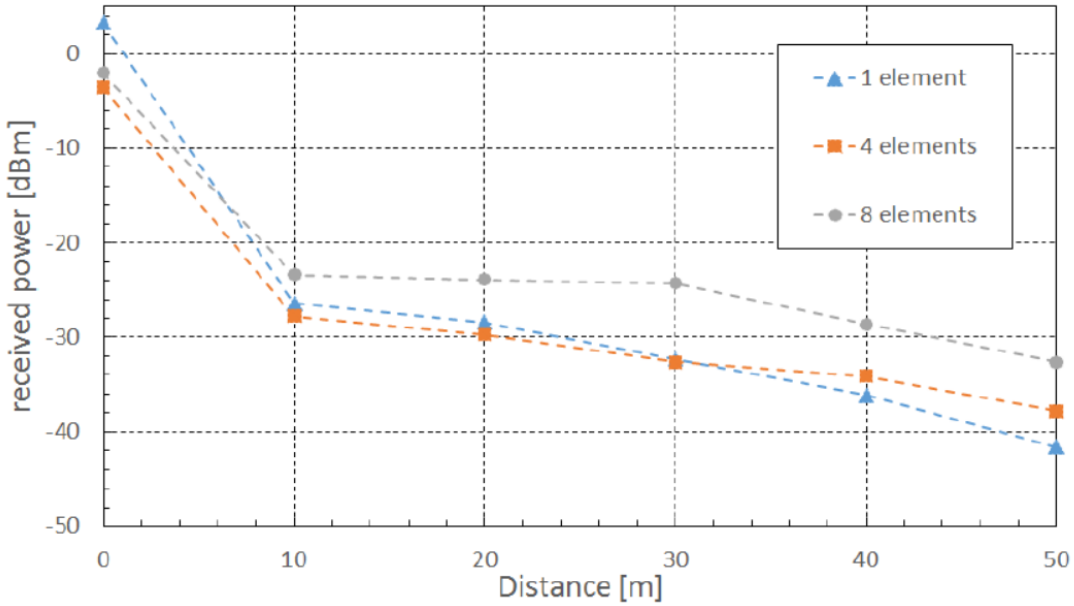

Figure 15 Relationship between distance and received power for array antennas with different elements composition

D. Simulation results

Fig. 16 and Fig. 17 show the simulation results of bit error rate and packet error rate using phased array antenna in the system, respectively. Evaluation parameters used in this simulation are given in Table 3. As depicted in Fig. 16, lower bit error rate of the proposed model is attainable at the high number of antenna elements. It is also found in Fig. 17 that with the deployment of a phased array antenna with 8 elements on the UAV, we can obtain a lower packet error rate compared to the UAV system without using the phased array antenna. What's more, the results also confirm that as the altitude of UAV increases, packet error rates also increase.

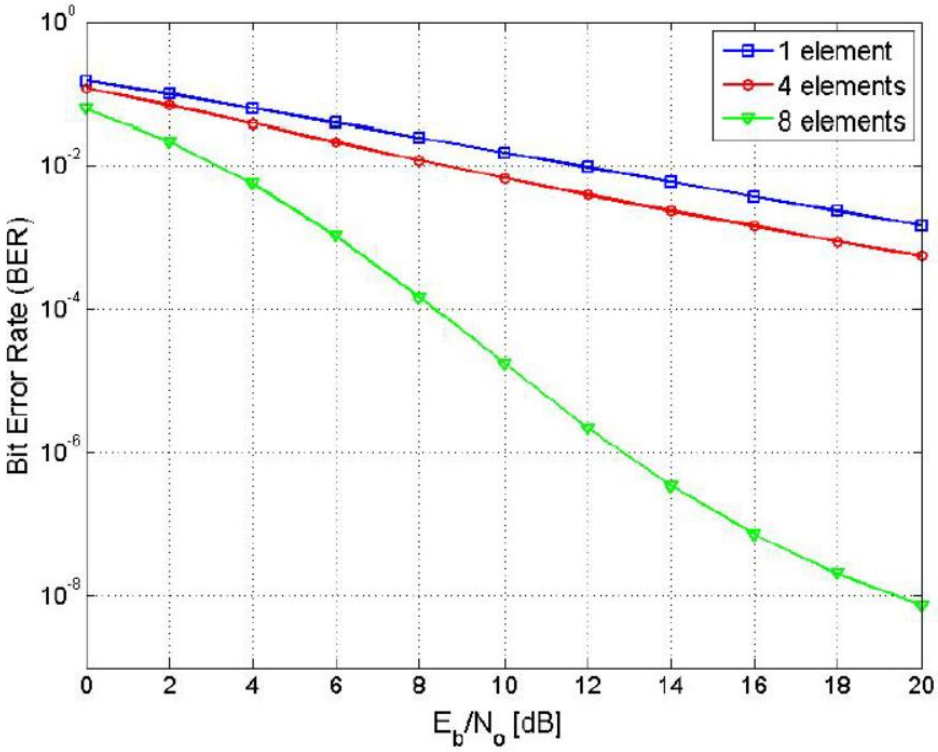

Figure 16 A comparison of an average Bit Error Rate (BER)

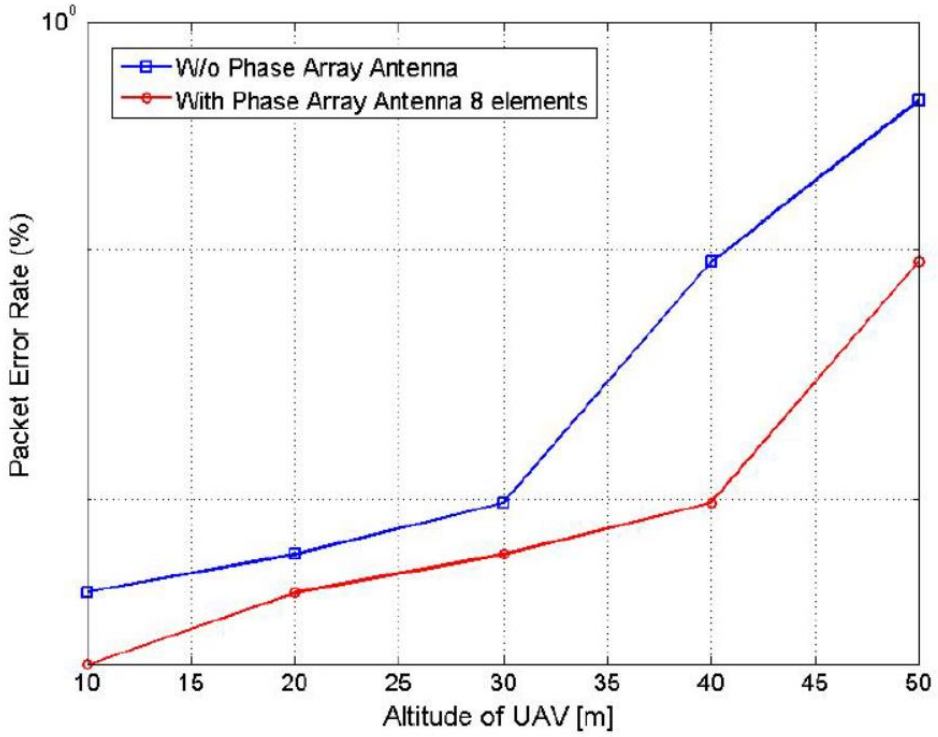

Figure 17 Packet Error Rate versus different altitudes of UAV

TABLE III Simulation parameters

Parameter	Value	Parameter	Value
UAV's speed	10 m/s	Frequency	2.4 GHz
UAV's altitude	10-50 m	Modulation Scheme	BPSK
# of elements	1-8	Channel model	Ricean fading
Packet size	25 Bytes	SNR	0-20 dB

● CONCLUSION

In view of the large number of missing people as a result of the Great East Japan Earthquake, we aim to construct a communication system to detect the missing people using the UAV which can quickly grasp a situation from the air when an existing communication infrastructure has broken down. We proposed the new systems which using the angle detector and the phased array antenna is able to steer the directivity to communicate in a wide area and over long distances. In this study, we performed various characteristic evaluations as the proposed system to aim to detect the missing people using the UAV. From the results of the UAV flight, we reaffirmed the need of our proposed system. Moreover, we made the phased array antenna which acts as the core of the system. We confirmed the advantage and its high functionality of the phased array antenna from the results. We confirmed the correlation between the received power level and the number of elements constituting the phased array antenna.

- REFERENCE

[1] Matthew O. Anderson, Scott G. Bauer, James R. Hanneman, and S. Shimamoto, Unmanned Aerial Vehicle (UAV) Dynamic-Tracking Directional Wireless Antennas for Low Powered Applications that Require Reliable Extended Range Operations in Time Critical Scenarios, in 2006 American Nuclear Society Meeting Proceedings, Feb.12-15, 2006.

[2] A. Khiewlamyong and C. Pirak, Loop Antenna Design for Smart Energy Meter, in Proc. of International Conference on Circuits, System and Simulation IPCSIT, vol. 7, 2011.

[3] K. Aso, N. Aomi, S. Sotheara, and S. Shimamoto, Study on Access schemes for Disaster Network System employing UAV., in Proc. of IEICE Technical Report, vol. 113, no. 456, pp. 527-532, 3-5 Mar. 2014

[4] Nobuo Mimura, Kazuya Yasuhara, Seiki Kawagoe, Hiromune Yokoki, and So Kazama, "Damage from the Great East Japan Earthquake and Tsunami - A quick report", Mitigation and Adaptation Strategies for Global Change October 2011, Volume 16, Issue 7, pp 803-818.

[5] S. Shimamoto, "Future Applications of UAV in Major Disaster based on Experience of Great East Japan Earthquake, Tsunami and Fukushima Nuclear Accident", Keynote, IEEE GLOBECOM Workshop on Wireless Networking for Unmanned Aerial Vehicles, TX, USA, Dec. 2011.

[6] Zou Yongqing, Cao Jun, and Cao Jun, Angle selection and dummy internal spacing methods for phased array antenna calibration based on travelling wave technology, Radar Conference, 2005 IEEE International.

[7] Richard C. Reinhart, Sandra K. Johnson, Dr. Roberto J. Acosta, and Dr. Scott Sands, Phased array antenna-based system degradation at wide scan angles, Phased Array Systems and Technology, 2003. IEEE International Symposium.

[8] S. Sotheara, K. Aso, N. Aomi, and S. Shimamoto, Effective Data Gathering and Energy Efficient Communication Protocol for Wireless Sensor Networks employing UAV., in Proc. of IEEE Wireless Communications and Networking Conference (IEEE WCNC), Istanbul, Turkey, Apr. 2014.

[9] ”Knowledge base, The Institute of Electronics, Information and Communication Engineers”, http://www.ieice-hbkb.org/portal/doc 586.html, 23Jun. 2015.

[10] S. Sotheara, N. Aomi, T. Ando, and S. Shimamoto, Circularly Multidirectional Antenna Arrays with Spatial Reuse based MAC for Aerial Sensor Networks., in Proc. of IEEE ICC, London, UK, Jun. 2015.

Field Experiment for Visualization of Radio Signal with UAV

Published in :, 2017, IEICE

● INTRODUCTION

Recently, it has been raised in importance about UAV which is an acronym for Unmanned Aerial Vehicle or Unmanned Automobile Vehicle. The UAV is an aircraft that flies without a human crew on board the aircraft and the UAV has so many types of small-size to large-size. The UAV can be roughly classified into type of fixed wing and type of rotary wing. Principal applications of the UAV are military, conveyance, aerial photography, disaster investigation, and etc. Originally the UAV has been used by military. For instance, the UAV has been used as a reconnaissance plane which name is a Global Hawk which type is fixed wing in America. However, recently, the UAV has been utilized in a board range of fields and caught a great attention in research fields. And in this paper, we focused on utility of UAV about investigation about visualization of the directivity of antennas.

In order to visualize the directivity of antennas, we assembled the system included UAV which type is rotary wing.

- **SYSTEM MODEL**

In order to visualize the directivity of antennas, we proposed the system which is contained eight detector circuits which are able to change received signal into LED light, eight received antennas which type is center-fed half-wave dipole antenna, and UAV. The proposed system is shown as Figure 18.The type of detector circuits of this system is half-wave double-voltage rectifier circuit which diagram. The half-wave double-voltage consists of two circuits: a clamper circuit and a peak detector (half-wave rectifier). The detector circuits of this system are composed of half-wave double-voltage rectifier circuits, resisters, and LED lights. The circuit catches the radio wave from the connected antenna, and the current flows in the LED right. If the radio wave strength which is received by this circuit is low, LED light shines weakly and vice versa.

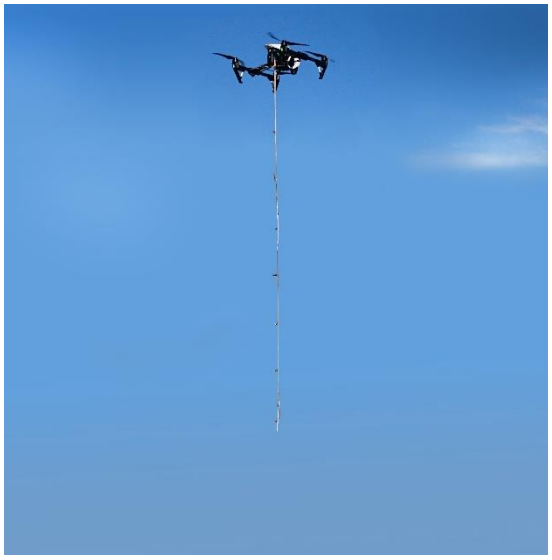

Figure 18 LED system with UAV

● EXPERIMENT

A. Experiment Set Up

We carried out an experiment to visualize the directivity of two antennas: Yagi-antennas which has 3 elements and 6 elements. At first, we measured the directivities of Yagi antenna which has 3 elements and 6 elements in anechoic chamber. The unit of measured directivity is decibel. However, in this experiment, we measured the directivity of antennas not logarithmically but linearly. So, we should change the directivity which unit is decibel into linear. To compare linear scale directivity of Yagi antenna with logarithm scale directivity, the linear and logarithm directivity of Yagi antennas which has 3 elements is shown as Figure 19 and 6 elements is shown as Figure 20. We carried out the experiment in kamogawa seminar house. The parameter of experiment is shown in table 1.

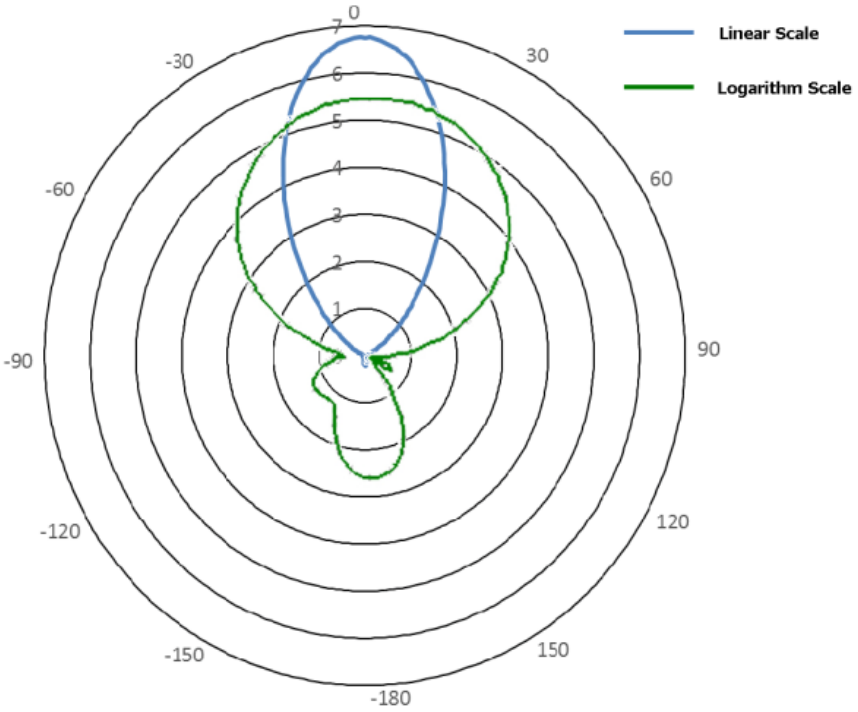

Figure 19 Comparison of directivity (3 elements)

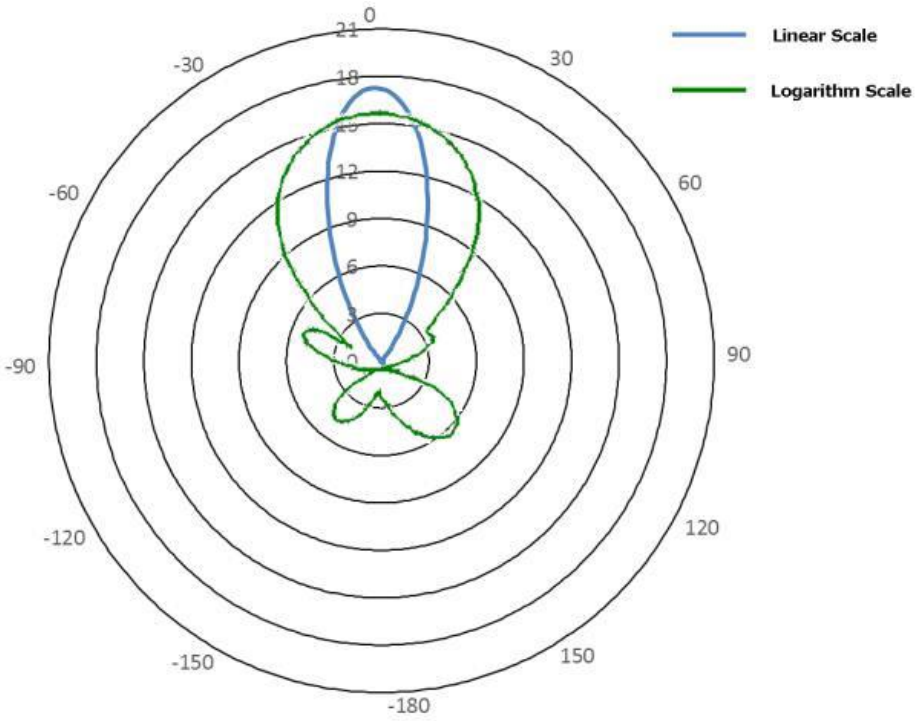

Figure 20 Comparison of directivity (6 elements)

Table 1 parameter of experiment

Transmitted power	20[W]
Frequency	435[MHz]
Height of Antenna	2.0[m]
Measured distance	7.0[m]
Measured interval	0.5[m]

B. Result

Figure 21 shows the comparison between the measured directivity of Yagi antenna which has 3 elements and measured liner directivity of 3 elements Yagi antenna which was obtained in anechoic chamber. And figure 22 shows the comparison between the measured directivity of Yagi antenna which has 6 elements and the measured liner directivity of 3 elements Yagi antenna which was obtained in anechoic chamber. The results are created and made to a three-dimension from Photoshop elements. We are able to recognize the difference between 3 elements and 6 elements. 6 elements received signal longer distance than 3 elements. And 3 elements lighted stronger than 6 elements at higher and lower point of near antennas.

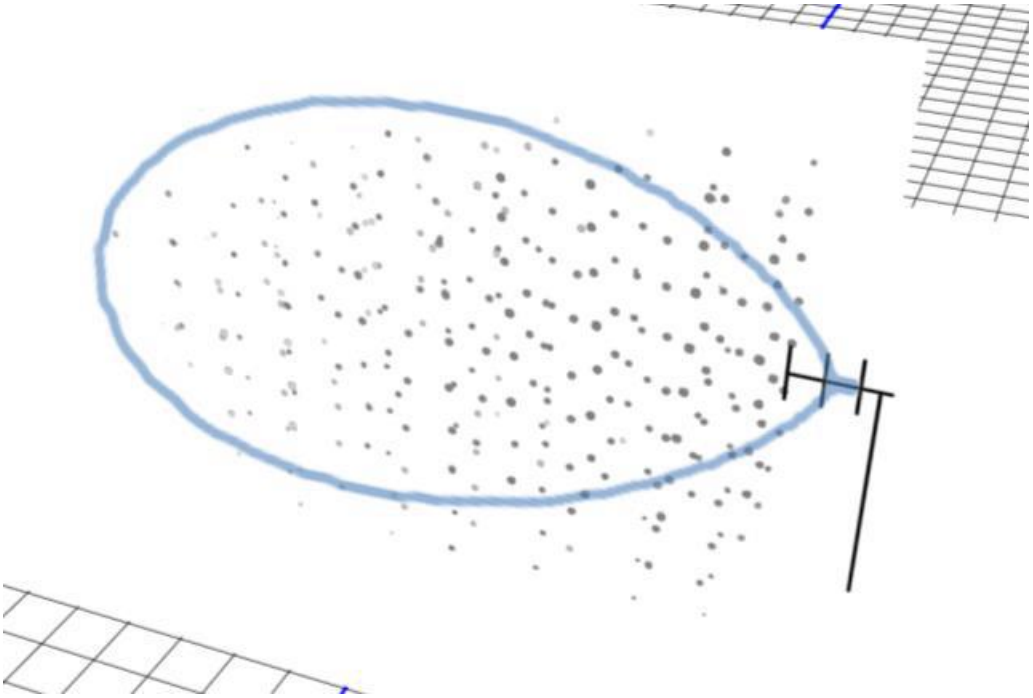

Figure 21 Result about directivity of Yagi antenna (3 elements)

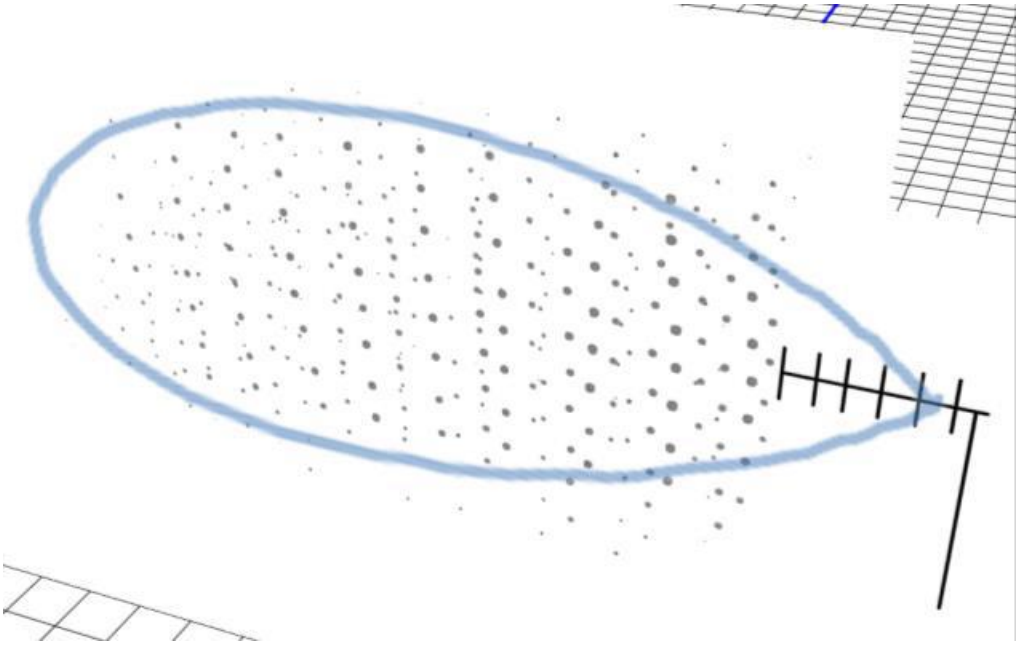

Figure 22 Result about directivity of Yagi antenna (6 elements)

● ANALYSIS

In order to check precision of the visualization system, we compare measurement date which was obtained in the real field with which was obtained in the anechoic chamber. We used the pearson correlation coefficient to check precision of the system. Using the following the formula, we check the relationship between the measurement data which was obtained in the real field and in the anechoic chamber.

$$r = \frac{\frac{1}{N}\sum_{i=1}^{N}(X_i - \bar{X})\,(Y_i - \bar{Y})}{\sqrt{\frac{1}{N}\sum_{i=1}^{N}(X_i - \bar{X})^2}\sqrt{\frac{1}{N}\sum_{i=1}^{N}(Y_i - \bar{Y})^2}}$$

Where r is pearson coefficient, N is number of data, X_i and Y_i is dataset;{x_1,…,x_n }{y_1,…,y_n }. Pearson coefficient r has value between +1 and -1inclusive, where +1 is positive correlation, 0 is no correlation, -1 is negative correlation. We calculated the correlation between the data in real field and in anechoic chamber using above formula, we obtained that average r is 0.62 for 3 elements, and average r is 0.67 for 6 elements. If 0<r<0.19, correlation is very weak. 0.2<r<0.39, is weak. 0.4<r<0.59, is moderate. 0.6<r<0.79, is strong. 0.8<r<1, is very strong.

CONCLUSION

We are able to illustrate the directivity of the antenna if we use the anechoic chamber. However, it is so difficult for us to illustrate the directivity of the antenna in the real fields. Therefore, we proposed and assembled the system which aim to be able to visualize the directivity of antennas in the real fields. In this experiment, we accomplished to assemble the visualization system and to visualize the directivity of antennas. View of experiment results, we confirmed the difference between Yagi antennas which has 3 elements and 6 elements. Comparing the experiment results and the simulation results using pearson correlation coefficient, average value is 0.62 (3 elements) and 0.67 (6 elements). Those values mean moderate match. The precision of the visualization system does not reach perfection. However, experiment results are close data with simulation one.

FUTURE WORK

The visualization system does not reach perfection. So we aim to improve the system and carry out more experiment in other situations.

- REFERENCE

[1] H. Inata, S. Say, T. Ando, J. Liu, S. Shimamoto," Unmanned Aerial Vehicle based Missing People Detection System employing Phased Array Antenna", IEEE WCNC workshop, Doha, Qatar, Apr. 2016

Research Achievement

- Hikari Inata, Sotheara Say, Taisuke Ando, Jian Liu, and Shigeru Shimamoto, *Unmanned Aerial Vehicle based on Missing People Detection System employing Phased Array Antenna*, Proc. of IEEE Wireless Communication and Networking Conference (WCNC) Workshop on Communicaions in Extreme Conditions, pp. 222-227, Doha, Qatar, April 2016.
- Hikari INATA Takayuki SAKAMOTO, Yukihiko OKOCHI, Liu ZHIBO, and Shigeru SHIMAMOTO, *Field Experiment for Visualization of Radio Signal with UAV*, the 2017 IEICE General Conference, March.
- Sotheara Say, Hikari Inata, Mohamad Erick Ernawan, Zhenni Pan, Jiang Liu, and Shigeru Shimamoto, *Partnership and Data Forwarding Model for Data Acquisition in UAV-aided Sensor Networks*, Proc. of IEEE Consumer Communications and Networking Conference (CCNC), Las Vegas, UAS, January 2017.
- Sotheara Say, Hikari Inata, and Shigeru Shimamoto, *A Hybrid Collision Coordination based Multiple Access Scheme for Super Dense Aerial Sensor Networks*, Proc. of IEEE Wireless Communication and Networking Conference (WCNC), pp. 1-6, Doha, Qatar, April 2016.
- Sotheara Say, Hikari Inata, Jiang Liu, and Shigeru Shimamoto, *Priority-based Data Gathering Framework in UAV-assisted*

Wireless Sensor Networks, IEEE Sensors Journal, Vol. 16, No. 14, pp. 5785-5794, July 2016

- Guangjie Chen, Ren Leshan, Hikari Inata, Liu Zhibo, and Shigeru Shimamoto, UAV automatic navigation and landing system, the 2016 IEICE General Conference.
- Taisuke Ando, Naoto Aomi, Hikari Inata, Jiang Liu, and Shigeru Shimamoto, *フェーズドアレイアンテナを用いた UAV 行方不明者探索システム*, The 2015 IEICE General Conference
- Naoto Aomi, Taisuke Ando, Hikari Inata, and Shigeru Shimamoto, *被災者捜索のためのマルチコプターUAV の編隊飛行を目的とした電波到来方向推定について*, The 2015 IEICE General Conference

Acknowledgements

First of all, I would like to express my greatest thanks to Prof. Shimamoto whose comments and suggestions were innumerably valuable throughout the course of my study.

Secondly, I would like to thank all members and friends in Shimamoto laboratory who always encourage and support me. Both of my study and daily life was fruitful because of them.

Thirdly, I would like to thank Prof. Tsujioka who is an associate professor at Osaka City University for corporation, feedbacks, and advices.

At last, I would also like to express my gratitude to my family for their big support and warm encouragements.

Reference

[1] Hikari Inata, Sotheara Say, Taisuke Ando, Jian Liu, and Shigeru Shimamoto, Unmanned Aerial Vehicle based on Missing People Detection System employing Phased Array Antenna, Proc. of IEEE Wireless Communication and Networking Conference (WCNC) Workshop on Communicaions in Extreme Conditions, pp. 222-227, Doha, Qatar, April 2016.

[2] Matthew O. Anderson, Scott G. Bauer, James R. Hanneman, and S. Shimamoto, Unmanned Aerial Vehicle (UAV) Dynamic-Tracking Directional Wireless Antennas for Low Powered Applications that Require Reliable Extended Range Operations in Time Critical Scenarios, in 2006 American Nuclear Society Meeting Proceedings, Feb.12-15, 2006.

[3] A. Khiewlamyong and C. Pirak, Loop Antenna Design for Smart Energy Meter, in Proc. of International Conference on Circuits, System and Simulation IPCSIT, vol. 7, 2011.

[4] S. Shimamoto, "Future Applications of UAV in Major Disaster based on Experience of Great East Japan Earthquake, Tsunami and Fukushima Nuclear Accident", Keynote, IEEE GLOBECOM Workshop on Wireless Networking for Unmanned Aerial Vehicles, TX, USA, Dec. 2011.

[5] K. Aso, N. Aomi, S. Sotheara, and S. Shimamoto, Study on Access schemes for Disaster Network System employing UAV., in Proc. of IEICE Technical Report, vol. 113, no. 456, pp. 527-532, 3-5 Mar. 2014

[6] Northrop Grumman Corporation, *Global Hawk*, Available at: <http://www.northropgrumman.com/Capabilities/GlobalHawk/Pages/default.aspx>, Accessed on December 10th 2016.

[7] AspenCore Inc., Voltage Multiplier Electronic Tutorials, Available at: <http://www.electronics-tutorials.ws/blog/voltage-multiplier-circuit.html>, Accessed on December 10th 2016.

[8] Tetsuo Tujioka, (n.d.), *ディジタルを楽しもう／JH1NRR 辻岡哲夫 第 6 回　簡易電界強度計を作る*, Available at: < http://www.fbnews.jp/201410/rensai/jh1nrr_digital_06_01.html>, Accessed on December 5th 2016.

[9] Peter Joseph Bevelacqua, (n.d.), *The Half-Wave Dipole Antenna Antenna-Theory.com*, Available at: <http://www.antenna-theory.com/antennas/halfwave.php>, Accessed on December 15th 2016.

[10] Peter Joseph Bevelacqua, (n.d.), *The Short Dipole Antenna Antenna-Theory.com*, Available at: <http://www.antenna-theory.com/antennas/shortdipole.php>, Accessed on December 12th 2016.

[11] Straw, Dean, N6BV, editor, The ARRL Antenna Handbook, 20th edition,The ARRL, Inc., Newington, CT, 2003

[12] Richard C. Johnson (1993), "ANTENNA ENGINEERING HANDBOOK third edition", MacGrraw-Hill, Inc.

[13] DJI Company Limited, *INSPIRE 1 specification* , Accessed at: <http://www.dji.com/inspire-1/info>, Accessed on January 13th 2017

[14] Peter Joseph Bevelacqua, (n.d.), *VSWR(Voltage Standing Wave Ratio) Antenna-Theory.com*, Available at: <http://www.antenna-theory.com/definitions/vswr.php>, Accessed on December 12th 2016.

[15] EIZO Corporation, 2010, About data of RGB and data of YUV, Available at: < http://www.eizo.co.jp/products/tech/files/2010/WP10-009.pdf>, Accessed on January 5th 2017.

[16] Pearson's Correlation, Available at: <http://www.statstutor.ac.uk/resources/uploaded/pearsons.pdf>, Accessed on January 5th 2017.

[17] *健康統計の基礎・健康統計学*, Last-modified: Tue, 11 Mar 2014, Available at: < http://hs-www.hyogo-dai.ac.jp/~kawano/HStat/?plugin=cssj&page=2010%2F4th%2FCorrelation>, Accessed on January 5th 2017.